

MINISTÈRE DE L'ENSEIGNEMENT SUPÉRIEUR ET
DE LA RECHERCHE SCIENTIFIQUE

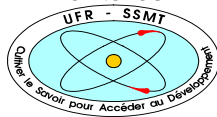
Felix Houphouët-Boigny university



No. 672



UNITÉ DE FORMATION ET DE
RECHERCHE SCIENCES DES
STRUCTURES DE LA MATIÈRE ET DE
TECHNOLOGIE



RÉPUBLIQUE DE CÔTE D'IVOIRE
UNION - DISCIPLINE - TRAVAIL
Institute of Energy and Climate Research –
Fundamental Electrochemistry (IEK-9),
Forschungszentrum Jülich



SPONSORED BY THE



**MASTER
IN RENEWABLE ENERGY AND CLIMATE CHANGE**

**SPECIALITY: PRODUCTION AND TECHNOLOGY OF GREEN
HYDROGEN**

MASTER THESIS:

Subject/Topic:

**MATERIAL CHARACTERISATION AND DESIGN OF DUAL PHASE STEEL
FOR HYDROGEN APPLICATION IN THE ENERGY SECTOR**

Presented on September 26, 2023 by:

Kelvin SARPONG

JURY:

Dr(MC) ZAHIRI Pascal

President

Dr AKRE Prisca

Examiner

Dr KOUAKOU Kouadio

Major Supervisor

Prof. Dr. -Ing. Ulrich Krupp

Co- Supervisor

ACADEMIC YEAR: 2022-2023

DEDICATION

I dedicate this work to God and everyone I crossed path with.

ACKNOWLEDGEMENT

I would like to express my sincere gratitude to all those who have contributed to the completion of this thesis. Their support, guidance, and encouragement have been invaluable throughout this journey.

First and foremost, I am deeply thankful to my thesis supervisors, Dr. Kouadio Kouakou and Prof. Ing. habil Ulrich Kr, for their unwavering support, expertise, and patience. Their mentorship and insightful feedback have been instrumental in shaping the direction and quality of this research.

I would also like to extend my appreciation to the members of my thesis jury committee, Dr. (MC) Zahiri Pascal and Dr. Akre Prisca, for their valuable input and constructive criticism. Their diverse perspectives have enriched this study.

I am grateful to the Federal Ministry of Education and Research (BMBF) for their financial support, which made this research possible. Their belief in the significance of this work has been a driving force behind my academic pursuits.

I owe a debt of gratitude to my family for their unwavering encouragement and belief in my abilities. Their love and support have been my constant motivation.

I am thankful to my friends and colleagues for their camaraderie, stimulating discussions, and moral support during the ups and downs of this academic journey.

To all those mentioned and countless others who have played a part in this endeavor, I offer my heartfelt thanks. Your contributions have left an indelible mark on this thesis, and I am deeply appreciative of your involvement.

ABSTRACT

The era of clean and sustainable energy transition is long overdue if net zero emissions by 2050 scenario is still the target, as per the Paris Agreement. Since the early 20's, intense research interests have been sparked in several aspects to explore the use of alternative energy source. Hydrogen is one of the clean and efficient energy carriers and it presents as a suitable zero emission fuel. It is one of the best chances to avoid drastic climate change effects by 2050, yet its storage, distribution, and transformation come with a major challenge limited by the interacting material's behaviour. This thesis focuses on the material characterisation and design for hydrogen application by analysing the hydrogen absorption rate of a dual-phase 980MPa by Slow Strain Rate Test (SSRT) and Thermal Desorption Spectroscopy (TDS) interactions under vary conditions of pressure, current density, and pressure., to understand design limitations and strategies for the materials for optimal usage for hydrogen in the energy sector.

The improvement in hydrogen-related material could improve the efficiency of hydrogen-related energy generation, transportation, and distribution. The research work starts with a comprehensive literature review on hydrogen embrittlement mechanism and its impact on structural and mechanical properties of metallic material (Dual phase steel). The various laboratory-induced hydrogen permeation, adsorption, hydrogen charging- electrochemical, and hydrogen measurement by Thermal Desorption Spectroscopy (TDS) alongside several other characterisation techniques for monitoring the effects and interactions of hydrogen, specifically Scanning Electron Microscopy (SEM). The findings from the TDS test will provide an insightful understanding of the hydrogen absorption rate of the dual-phase steel, kinetics of hydrogen's interactions, microstructural changes, and behaviour of hydrogen-induced degradation on mechanical properties of metallic materials.

The research findings provide insightful knowledge of the behaviour of the metallic material in hydrogen environments, and this will aid in the design of materials robust and efficient for hydrogen application in the energy sector.

Keywords: hydrogen embrittlement; hydrogen absorption rate; hydrogen charging; dual phase steel (ferrite, martensite) phase equilibrium; energy sector.

RÉSUMÉ

L'ère de la transition énergétique propre et durable est attendue depuis longtemps si le scénario de zéro émission nette d'ici 2050 reste l'objectif, conformément à l'Accord de Paris. Depuis le début des années 20, d'intenses intérêts de recherche ont été suscités sous plusieurs aspects pour explorer l'utilisation de sources d'énergie alternatives. L'hydrogène est l'un des vecteurs d'énergie propres et efficaces et se présente comme un carburant approprié à zéro émission. C'est l'une des meilleures chances d'éviter les effets drastiques du changement climatique d'ici 2050, mais son stockage, sa distribution et sa transformation posent un défi majeur limité par le comportement des matériaux en interaction. Cette thèse se concentre sur la caractérisation et la conception de matériaux pour les applications de l'hydrogène en analysant le taux d'absorption d'hydrogène d'un 980 MPa biphasé par des interactions de test de vitesse de déformation lente (SSRT) et de spectroscopie de désorption thermique (TDS) dans diverses conditions de pression, de densité de courant et pression., pour comprendre les limites de conception et les stratégies des matériaux pour une utilisation optimale de l'hydrogène dans le secteur de l'énergie.

L'amélioration des matériaux liés à l'hydrogène pourrait améliorer l'efficacité de la production, du transport et de la distribution d'énergie liée à l'hydrogène. Le travail de recherche commence par une revue complète de la littérature sur le mécanisme de fragilisation par l'hydrogène et son impact sur les propriétés structurales et mécaniques des matériaux métalliques (acier double phase). Les différentes perméations d'hydrogène, adsorption, charge d'hydrogène - électrochimiques et mesures d'hydrogène induites en laboratoire par spectroscopie de désorption thermique (TDS) ainsi que plusieurs autres techniques de caractérisation pour surveiller les effets et les interactions de l'hydrogène, en particulier la microscopie électronique à balayage (MEB). Les résultats du test TDS fourniront une compréhension approfondie du taux d'absorption de l'hydrogène de l'acier biphasé, de la cinétique des interactions de l'hydrogène, des changements microstructuraux et du comportement de la dégradation induite par l'hydrogène sur les propriétés mécaniques des matériaux métalliques.

Les résultats de la recherche fournissent des connaissances approfondies sur le comportement des matériaux métalliques dans les environnements hydrogène, ce qui facilitera la conception de matériaux robustes et efficaces pour les applications de l'hydrogène dans le secteur de l'énergie.

Mots clés : fragilisation par l'hydrogène ; taux d'absorption de l'hydrogène ; chargement d'hydrogène; équilibre des phases d'acier à deux phases (ferrite, martensite); secteur énergétique.

Table of Contents

DEDICATION	1
ACKNOWLEDGEMENT	ii
ABSTRACT	iii
RÉSUMÉ	iv
ACRONYMS AND ABBREVIATIONS	xi
1. INTRODUCTION	1
1.1 Climate Crisis	1
1.2 Energy Transition	1
1.3 Hydrogen As An Energy Carrier	1
1.3.1 Hydrogen Transportation In The Energy Sector	2
1.4 Design Strategies and Limitations	2
1.5 Objective	3
2. LITERATURE REVIEW	4
2.1 Energy Consumption by The Energy Sector	4
2.2 Why Hydrogen?	5
2.3 Challenges In Using Hydrogen	5
2.4 First-Generation Steels	7
2.4.1 Dual phase steels	7
2.4.2 Complex phase steels	7
2.4.3 TRIP steel	9
2.4.4 Martensitic steel	9
2.5 Hydrogen Mechanisms	11
2.6 Green Steel For Hydrogen Application	12
2.7 Hydrogen Pipeline Operation In The Energy Sector	12
2.8 Hydrogen Absorption And Transport In Steels	13
2.8.1 Hydrogen absorption	13
2.8.2 Hydrogen' solubility and diffusivity in steels	13
2.8.3 Hydrogen- induced defects and cracks in steels	15
2.8.4 Hydrogen embrittlement	15
2.8.5 The mechanism of Hydrogen-induced Cracking	17

2.9 Material Characterization Techniques for DP Steel	19
2.10 Hydrogen charging methods	21
2.11 Alloying design for Hydrogen Compatibility	22
2.12 Phase Equilibrium of DP Steel during interaction with Hydrogen	23
2.13 Importance of alloying methods in Hydrogen application	24
2.14 Hydrogen Storage and Transportation Mechanisms and Technologies	28
3 MATERIALS AND EXPERIMENTAL METHODS	30
3.1 Examined Material and its composition.	30
3.2 Hydrogen charging and analysis	30
3.2.1 Thermal Desorption Spectroscopy	30
3.3 Thermal Desorption Spectroscopy measurement	32
4 CHARACTERISATION OF DUAL PHASE MATERIAL	34
4.1 Chemical Composition Of The DP980MPa	34
4.2 Microstructure characterisation	34
4.3 Characterisation of Dual-Phase Steel Material	35
5. DISCUSSION OF HYDROGEN'S INFLUENCE ON MECHANICAL PROPERTIES	36
5.1 Discussion of results from Thermal Desorption Spectroscopy	36
5.1.1 Without Charging	36
5.1.2 Thermal Desorption Spectroscopy at 0.2mA/cm ² in 1hour with 0MPa	37
5.1.3 Thermal Desorption Spectroscopy at 0.02mA/cm ² in 1 hour with 0MPa	38
5.1.4 Thermal Desorption Spectroscopy at 2mA/cm ² in 1 hour with 0MPa	40
5.1.5 Thermal Desorption Spectroscopy at 0.2mA/cm ² in 1 hour with 50MPa	41
5.1.6 Thermal Desorption Spectroscopy at 0.2m/cm ² in 1hour with 100MPa	42
5.1.7 Thermal Desorption Spectroscopy at 0.2m/cm ² in 1hour with 150MPa	43
5.1.8 Thermal Desorption Spectroscopy at 0.2m/cm ² in 1hour with 300MPa	44
5.1.9 Thermal Desorption Spectroscopy at 0.2m/cm ² in 1hour with 600MPa	45
5.2.0 Combined results of all TDS graphs	46
5.2.1 Combined results of all TDS graphs with time as the x axis	47
5.3 Analysis of results from TDS	47
5.3.1 Temperature	47
5.3.2 Pressure	48
5.3.3 Charging densities	48
5.3.4 Combined effects	48

5.4 Evaluation of the susceptibility to HE and the consequences of using Dual Phase Steel for hydrogen application in the energy sector	48
6. CONCLUSION AND RECOMMENDATION	50
REFERENCE	52

LIST OF TABLE

TABLE 1: COMPOSITION IN WEIGHTED PERCENTAGES OF ALLOYED INVESTIGATED [17].....	18
TABLE 2: LIST OF ALL THE DUAL-PHASE STEELS AND THE VARYING CONDITIONS	33
TABLE 3: LIST OF ALL THE CHEMICAL PROPERTIES IN WEIGHTED PERCENTAGES OF THE DUAL-PHASE STEEL MATERIAL USED	34

LIST OF FIGURES

FIGURE 1: MICROSTRUCTURE OF THE FIRST-GENERATION STEELS WITH THEIR RESPECTIVE COMPONENTS [123]	6
FIGURE 2: IRON/CARBON ALLOY PHASE DIAGRAM [122]	10
FIGURE 3: STRENGTH AGAINST ELONGATION GRAPH DEPICTING THE RANGE OF PROPERTIES FOR ALL KNOWN STEELS. [121].....	11
FIGURE 4: PRESENTATION OF ALL KNOWN DEFECTS IN METALS AND THEIR INTERACTION WITH HYDROGEN ATOMS.....	11
FIGURE 5: A FIGURE ILLUSTRATING HYDROGEN DIFFUSION TOWARDS REGION OF HIGHER HYDROSTATIC STRESS.	14
FIGURE 6: A DESCRIPTION OF SOLUBILITY OF HYDROGEN IN STEELS []	15
FIGURE 7: HYDROGEN EMBRITTLEMENT SUMMARY []	15
FIGURE 8: HYDROGEN EMBRITTLEMENT REACTION PROCEDURE [78]	19
FIGURE 9: HYDROGEN ABSORPTION ON DP STEELS WITH AND WITHOUT COATING [124]	23
FIGURE 10: EFFECT OF TEMPERATURE, CHARGING CURRENT DENSITY AND PHASE COMPOSITION [121]	24
FIGURE 11: PHENOMENON BEHIND TDS EXPERIMENT []	31
FIGURE 12: TDS SUMMARY.....	31
FIGURE 13: A GRAPH OF TDS SHOWING THE EFFECT OF CHARGING ON HYDROGEN ABSORPTION RATE [].....	32
FIGURE 14: MICROSTRUCTURE OF DP980 AT FOUR DIFFERENT MAGNIFICATIONS	34
FIGURE 15: A TYPICAL SHAPE DP STEEL FOR THE EXPERIMENT	35
FIGURE 16: TDS GRAPHS (1&2) OF HYDROGEN DESORPTION RATE IN PPM/S AGAINST TEMPERATURE IN KELVIN OF A DP980 WEIGHTED 11.956G WITHOUT CHARGING RECORDED IN THE LABORATORY.	36
FIGURE 17:A TDS GRAPH OF HYDROGEN DESORPTION RATE IN PPM/S AGAINST TEMPERATURE IN KELVIN OF A DP980 WEIGHTED 11.93G WITHOUT CHARGING RECORDED IN THE LABORATORY	36
FIGURE 18:A TDS GRAPH OF HYDROGEN DESORPTION RATE IN PPM/S AGAINST TEMPERATURE IN KELVIN OF A DP980 WEIGHTED 12.2154G.....	37
FIGURE 19: A TDS GRAPH OF HYDROGEN DESORPTION RATE IN PPM/S AGAINST TEMPERATURE IN KELVIN OF A DP980 WEIGHTED 12.1728G RECORDED IN THE LABORATORY	37
FIGURE 20:A TDS GRAPH OF HYDROGEN DESORPTION RATE IN PPM/S AGAINST TEMPERATURE IN KELVIN OF A DP980 WEIGHTED 12.184G RECORDED IN THE LABORATORY	38
FIGURE 21:A TDS GRAPH OF HYDROGEN DESORPTION RATE IN PPM/S AGAINST TEMPERATURE IN KELVIN OF A DP980 WEIGHTED 12.1523G RECORDED IN THE LABORATORY.	38
FIGURE 22:A TDS GRAPH OF HYDROGEN DESORPTION RATE IN PPM/S AGAINST TEMPERATURE IN KELVIN OF A DP980 WEIGHTED 12.1833G RECORDED IN THE LABORATORY	39
FIGURE 23:A TDS GRAPH OF HYDROGEN DESORPTION RATE IN PPM/S AGAINST TEMPERATURE IN KELVIN OF A DP980 WEIGHTED 12.148G RECORDED IN THE LABORATORY.	39
FIGURE 24:A TDS GRAPH OF HYDROGEN DESORPTION RATE IN PPM/S AGAINST TEMPERATURE IN KELVIN OF A DP980 WEIGHTED 12.247G RECORDED IN THE LABORATORY.	40
FIGURE 25: A TDS GRAPH OF HYDROGEN DESORPTION RATE IN PPM/S AGAINST TEMPERATURE IN KELVIN OF A DP980 WEIGHTED 12.2086G RECORDED IN THE LABORATORY.	40
FIGURE 26: A TDS GRAPH OF HYDROGEN DESORPTION RATE IN PPM/S AGAINST TEMPERATURE IN KELVIN OF A DP980 WEIGHTED 12.2458G RECORDED IN THE LABORATORY.	41
FIGURE 27: A TDS GRAPH OF HYDROGEN DESORPTION RATE IN PPM/S AGAINST TEMPERATURE IN KELVIN OF A DP980 WEIGHTED 2.3134G RECORDED IN THE LABORATORY.	41
FIGURE 28:A TDS GRAPH OF HYDROGEN DESORPTION RATE IN PPM/S AGAINST TEMPERATURE IN KELVIN OF A DP980 WEIGHTED 2.6053G RECORDED IN THE LABORATORY.	42
FIGURE 29:A TDS GRAPH OF HYDROGEN DESORPTION RATE IN PPM/S AGAINST TEMPERATURE IN KELVIN OF A DP980 WEIGHTED 2.079G RECORDED IN THE LABORATORY.	42
FIGURE 30: A TDS GRAPH OF HYDROGEN DESORPTION RATE IN PPM/S AGAINST TEMPERATURE IN KELVIN OF A DP980 2.0851G RECORDED IN THE LABORATORY.....	43
FIGURE 31: A TDS GRAPH OF HYDROGEN CONTENT IN PPM/S AGAINST TEMPERATURE IN KELVIN OF A DP980 WEIGHTED 2.5282G RECORDED IN THE LABORATORY.	43

FIGURE 32: A TDS GRAPH OF HYDROGEN DESORPTION RATE IN PPM/S AGAINST TEMPERATURE IN KELVIN OF A DP980
WEIGHTED 2.5281G RECORDED IN THE LABORATORY.44

FIGURE 33: A TDS GRAPH OF HYDROGEN DESORPTION RATE IN PPM/S AGAINST TEMPERATURE IN KELVIN OF A DP980
WEIGHTED 2.662G RECORDED IN THE LABORATORY.44

FIGURE 34: A TDS GRAPH OF HYDROGEN DESORPTION RATE IN PPM/S AGAINST TEMPERATURE IN KELVIN OF A DP980
WEIGHTED 2.2165G RECORDED IN THE LABORATORY.45

FIGURE 35: A TDS GRAPH OF HYDROGEN DESORPTION RATE IN PPM/S AGAINST TEMPERATURE IN KELVIN OF A DP980
2.3384G RECORDED IN THE LABORATORY.....45

FIGURE 36: A TDS GRAPH OF HYDROGEN DESORPTION RATE IN PPM/S AGAINST TEMPERATURE IN KELVIN OF A DP980
2.2254G RECORDED IN THE LABORATORY.....46

FIGURE 37: A TDS GRAPH OF ALL THE COMBINED VARYING CONDITIONS FOR HYDROGEN DESORPTION RATE IN PPM/S AGAINST
TEMPERATURE IN KELVIN.46

FIGURE 38: A TDS OF ALL THE COMBINED VARYING CONDITIONS FOR HYDROGEN DESORPTION RATE IN PPM/S AGAINST TIME IN SECOND.47

ACRONYMS AND ABBREVIATIONS

AHSS:	Advanced High Strength Steel
COP:	Conference of Parties
CP:	Complex Phase
DP:	Dual Phase
EJ:	Exajoule
HAR:	Hydrogen Absorption Reaction
HEAC:	Hydrogen Environment Assisted Cracking
HER:	Hydrogen Evolution Reaction
HIC :	Hydrogen-Induced Cracking
IEA:	International Energy Agencies
IHAC:	Internal Hydrogen Assisted Cracking
MDG :	Millennium Development Goals
MPa:	Mega Pascal
SEM:	Scanning Electron Microscopy
SDI :	Spatial Data Infrastructure
TDS:	Thermal Desorption Spectroscopy
TRIP:	Transformation Induced Plasticity effect
UN:	United Nation
UNFCCC:	United Nation Framework Convention on Climate Change
UTS:	Ultimate Tensile Strength
WASCAL :	West African Science Service Center on Climate Change and Adapted Land Use
WHO :	World Health Organization

1. INTRODUCTION

1.1 Climate Crisis

Over the years, there have been conspicuous and consistent concerns about climate change, to the extent that the public and media are noticeably involved in creating awareness and demanding adaptive and mitigative measures, and the need for imminent combative measures. Today's energy exploitation, production, distribution, and usage contribute massively climate crisis. The energy sector, in 2021, accounted for the majority- 76% of greenhouse gases produced [1], the major climate driver. Simultaneously, at the current population growth rate likewise the staggering modernity growth pace this fraction will surge even higher in the few years ahead. This course will make the achievement of the Paris Agreement's goal - keeping the global average temperature rise in this century as close as possible to 1.5°C above pre-industrial levels- difficult to achieve. Thus, the energy transition agenda has become eminent more than ever as agreed on at the COP 26 'Glasgow significantly picks up the pace on climate action – and urgency is key' as noted by Federal Environment Minister Svenja Schulze.

1.2 Energy Transition

The IEA, being at the heart of global energy dialogues, is consistently bringing to light global energy usage and its effect on the globe. All stakeholders have important roles to play in this campaign, through policies, funding research, development, and technology. Consequently, Climate Change Conferences that are being held through Paris Agreement UNFCCC consistently inform on energy crisis and its progress and to promote the need to be more sustainable in their regards. These conferences over the years have addressed the need to adopt clean energy measures at the core of energy transition.

To achieve IEA'S Net Zero Emission by 2050 Scenario, adopting the utilization of clean energy assures the globe of sustainable survival, amongst these proposals are: renewable energy such as wind and water, increasing energy efficiency; electrifying transport, industry, and buildings; expanding the use of clean hydrogen and other low-emission fuels; and investing in emission abating technologies, including negative emission technologies. Ever since the affirmation of the assertion for the usage of clean and sustainable energy was made [2], there have been monotonous thriving interests in research giving way to daunting technologies. Amid this discussion, the ideal way to achieve the Net Zero Emission scenario requires energy transition to a low-carbon fuel hydrogen energy is being presented as the best option.

1.3 Hydrogen as An Energy Carrier

Hydrogen is an ideal zero-carbon fuel and the prospect reaching the net zero agenda. The utilization of hydrogen, as a promising fuel, has the potential to combat climate crisis [3]. It poses several advantages, including its relatively high energy density, environmental climate friendliness, and compatibility with

various energy conversion systems such as fuel cells with high efficiency [4]. These make it competitive for various applications such as transportation, power generation, and ‘timely’ energy storage. Though it comes with these undisputed advantages, the implementation of this carbon-neutral fuel has been limited by hydrogen embrittlement affecting storage and transport of hydrogen through metallic material for several applications.

1.3.1 Hydrogen Transportation In The Energy Sector

The utilization of hydrogen as an energy carrier in the energy sector has great potential to drastically reduce the global warming arising from that sector. The material grades for application in this sector are still being investigated. It is greatly being posed by one great limitation, hydrogen embrittlement, thus the main motive for this thesis.

1.4 Design Strategies and Limitations

Material characterisation and design strategies are pertinent to assist in the recommendation of safe and efficient utilization of hydrogen in diverse application. This research work will primarily investigate the hydrogen absorption potential, crystal lattice behaviour, and microscopic properties of dual-phase steel materials and their interaction with hydrogen and propose design recommendations and approaches for hydrogen applications in the energy sector. The research aims to address fundamental aspects related to hydrogen embrittlement mechanisms, hydrogen charging, hydrogen measurement, phase equilibrium, and interaction of hydrogen with dual-phase steels.

Hydrogen embrittlement, a significant concern in structural materials, refers to the phenomenon where the presence of hydrogen induces unexpected degradation and fracture in metals lattice [5]. The understanding of these mechanisms of hydrogen embrittlement is essential for developing strategies to mitigate its detrimental effects on dual-phase steel materials. This research will involve a comprehensive investigation of hydrogen embrittlement mechanisms through hydrogen absorption and diffusion in a dual-phase steel, and its observed resultant microstructural changes using advanced characterization techniques: Thermal Desorption Spectroscopy (TDS) and Scanning Electron Microscopy (SEM). To assess the susceptibility of dual-phase steel to hydrogen-induced degradation, hydrogen charging experiments will be conducted using electrochemical methods. These experiments will provide insights into the effects of hydrogen on the corrosion behavior and mechanical integrity of dual-phase steel materials, to contribute to the development of robust materials resistant to hydrogen embrittlement. Furthermore, this research will explore the phase equilibrium- the interactions of ferrite and martensite phases with hydrogen through phase diagrams. Through the investigation of the influence of alloying elements, and surface coating on hydrogen absorption and embrittlement, novel materials can be designed with enhanced resistance to hydrogen-induced

degradation. This will pave the way for the development of advanced alloys suitable for hydrogen storage and transportation applications or hydrogen application in the energy sector.

1.5 Objective

The findings of this thesis will contribute to the understanding of hydrogen desorption rate by Thermal Desorption Spectroscopy under varying conditions of pressure, temperature, and current density and eventually to understand the hydrogen-material (DP steel) interactions, the design of materials (DP steel) for hydrogen applications, and the advancement of hydrogen-based technologies in the energy sector. The outcomes are expected to provide valuable insights and recommendations for material characterization, alloy design, and engineering practices aimed at optimizing the performance, reliability, and safety of hydrogen-related systems for their application in the energy sector.

Overall, this research represents a significant step towards enabling the widespread adoption of hydrogen as a clean and sustainable energy source fostering progress in the field of material characterization and design for hydrogen application.

2. LITERATURE REVIEW

The urgent problems of climate change, air pollution, and heightened conventional resource depletion as well as its price escalations since 2020 have made the energy transition to sustainable and clean energy sources significant on a global scale, because of the increasing importance of ecological restrictions. For the incoming generations, renewable energy sources will be their main means of supplementing their energy requirements. It is expected to be a common feature that will substantially change the face of energy exploration spatially owing to their geographical availability. Renewable energy exploration is devoid of carbon and sulfur and contains none of the pollutants that have already led to the restriction of hydrocarbons. The intensive act to phase-out of nuclear energy has made the exploration of some renewable energies such solar energy on extensive scale to achieve the global energy requirement. To fully supply the global energy requirements, there should be the incorporation of other energy carriers to solve the issues of loss in storage and distribution since solar energy has economic limitation in being transported over great intercontinental distances. This is unfortunately one of the economic limitations of the fossil energy system.

2.1 Energy Consumption by The Energy Sector

Preeminently, IEA [6] reports that World energy production amounted to 617 EJ in 2019 – a 2% increase from 2018. This increase was mostly driven by natural gas (+4%) and coal (+2%), though some renewables increased much more in relative terms (e.g., +14% for solar and +12% for wind). Hydro-electricity production stagnated at 15 EJ. While it did not increase in 2019, oil remained the most produced form of energy, at 190 EJ. Fossil fuels accounted for more than 81% of production in 2019, as in the previous years. This energy production amount is subject to about 21% increase 2040. The world would need twice as much energy as it produces today if it were not for continuous improvements in energy efficiency, this era is no different as a result there is no time to blink an eye over energy issues, as the emerging markets and fast developing economies will present an increase in energy demand. If the Net Zero remains the target as conspicuously discussed in COP26 in Glasgow, renewable energies have a huge gap to fill thus it must be weighed against optimal storage and transportation. The storage and transportation potential raises lots of questions marks. If the zero-carbon economy is prioritized in achieving our energy requirements there must be a complementary energy alternative. Amongst the various promising alternative energy carriers' options, lots of emphasizes are being placed on the mentions of hydrogen – hydrogen has been proven to be the energy of the future by its ability to be essentially stored and transported in liquid and gaseous form consequently improving the energy storage and transportation potential and to also its availability to balance the fluctuations in energy production and consumption [7]. Energy storage and transportation are paramount in the improvement of harvested renewable energy to offer the balance in production and consumption [8], as it is the excellent path to aligning with the Net Zero Emission scenario, along with its high energy density.

Thus, it has garnered significant attention as a viable solution for achieving the net-zero scenario by 2050 [9].

2.2 Why Hydrogen?

Besides hydrogen's competitive characteristics, which makes it earn the name "fuel of the future", it is accustomed that it can be produced from variety of renewable energy sources such as electrolysis powered by solar or wind energy, which notable especially in the interest of sustainability since it produces no carbon, sulfur, dust particles or heavy metals [10]. These renewable production pathways make hydrogen's sustainability and environmental friendliness a great concern in the decarbonization agenda because it does not produce any carbon monoxides and dioxides and ultimately the by-product is a significant product that offers essential usage - oxygen. Likewise, hydrogen has the potential of being stored and transported, which will enable efficiency in distribution and supply upon request across different sectors and remote areas-areas where traditional conventional electricity may not be available. Consequently, it has a plethora of potential uses. In the automobile industry, the longer driving ranges, quicker refueling periods, and less noise pollution make hydrogen fuel cell vehicles attractive alternative to traditional internal combustion engines [11]. In industries like steel production and heavy-duty manufacturing, where direct electrification is difficult, hydrogen can play a critical role in decarbonizing businesses through the operation of electrolyzes and liquefaction plants. Hydrogen can also be used for grid balancing, energy storage, and decentralized power generation, helping to integrate renewable energy sources and guarantee a consistent and stable power supply [12]

2.3 Challenges In Using Hydrogen

Despite hydrogen's immense potential as an energy source, there are still several pressing problems that must be overcome. Before being fully integrated into the energy sector, the safety of hydrogen during its usage and operation must be appropriately limited to ensure that it checks every safety box. Despite being well-known for a long time, hydrogen lacks several safety precautions, which has delayed its full operations in many sectors, and the safety requirements are continually being updated. Hydrogen has been found to exhibit a wide range of flammability, low ignition energy, relatively high flame velocity, quick diffusion, and buoyancy in a laboratory investigation [13]. Hydrogen is odorless, very flammable, and produces colorless flames when it is in the liquid state [14]. Increasing energy efficiency, lowering costs, keeping hydrogen purity, and minimizing hydrogen leakage are the key risks that are behind these. When a chemical with these qualities leaks, it would result on severe catastrophe. With the growth of hydrogen consumption technology and the development of affordable and efficient hydrogen production techniques, the issue of hydrogen embrittlement is frequently faced in the construction of trustworthy infrastructure for storage and distribution. Safety issues and public acceptance must be adequately handled in all applications if hydrogen

is to be used widely as an energy source. For use in the energy sector, the dual-phase steel mechanism's design and material characterization will be extensively examined.

At 1 atm pressure and 0°C temperature, hydrogen has a mass per gallon of 0.00075 kg, making it the lightest element by a wide margin. Hydrogen needs to be compressed or liquified and transported under pressure to be distributed efficiently [15]. Today, hydrogen is delivered by pipelines, cryogenic liquid tanker trucks, or gaseous tube trailers from production facilities to customers [16]. In extensive applications, different chemical carriers have been proposed. Additional infrastructure, such as compression, storage, dispensers, meters, containment detection, and purification technologies, is frequently utilized at the consumer's end of the operation. In the energy sector, the following methods are typically utilized to supply hydrogen: as gaseous hydrogen in pipelines and tube trailers; as liquid hydrogen in new hydrogen carriers; as bulk hydrogen stored on-site; and as hydrogen fuel dispensed to automobiles. Most significantly, extensive research is being done on the material employed for this application and its interactions.

Climate seminars in the energy sector warn against high CO_2 emissions rates in the steel development and application technologies. Analysis and consideration were given to the first generation of advanced high-strength steels (AHSS), which consists of typical ferritic multiphase steels with ferrite-based microstructure. The first generation of AHSS includes martensitic (MS) steels, dual-phase (DP) steels, complex phase (CP) steels, and steels with transformation-induced plasticity (TRIP).

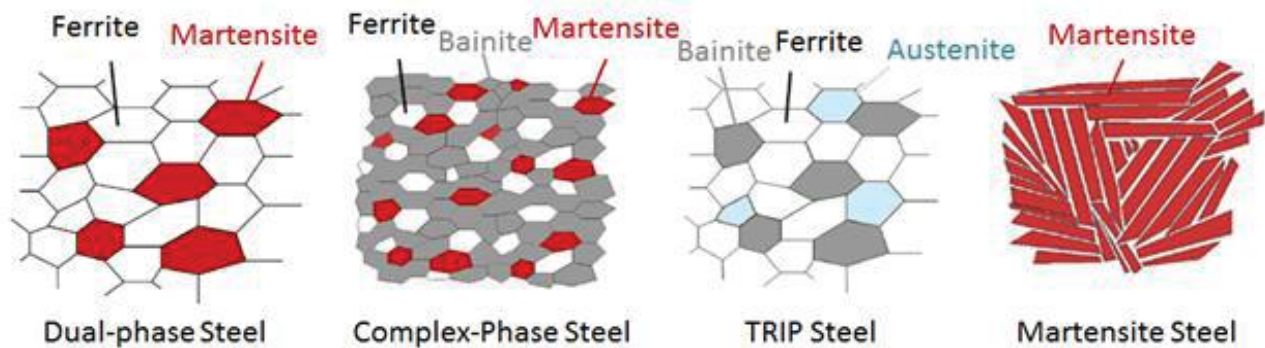


Figure 1: Microstructure of the first-generation steels with their respective components [123]

2.4 First-Generation Steels

2.4.1 Dual phase steels

The dual-phase steels will be thoroughly explored for their hydrogen absorption rate by TDS for this study. High-strength steel with a ferritic-martensitic microstructure is known as Dual Phase (DP) steel. Low or medium-carbon steels are used to make DP steels, which are quenched at a temperature that is higher than A1 but lower than A3 according to a continuous cooling transformation diagram [17]. As a result, a microstructure is formed that is made up of islands of martensite, a secondary phase that boosts tensile strength, within a soft ferrite matrix. As a result, the volume fraction, morphology (size, aspect ratio, interconnectivity, etc.), grain size, and carbon content all influence how DP Steels behave overall.

DP steels typically contain 0.06–0.15% C and 1.5–3% Mn (the former strengthens the martensite and the latter causes solid solution strengthening in ferrite, while both stabilize the austenite), along with Si (to promote ferrite transformation), V, and Nb (for precipitation strengthening and microstructure refinement) as well as Cr & Mo (to retard pearlite or bainite formation) [18]. The martensite in the DP steels allows for high ultimate tensile strength (UTS) [17], which is combined with low initial yielding stress, high early-stage hardening, and microscopically uniform plastic flow (all made possible by the lack of Luders effect).

Due to these characteristics, DP steels are most frequently employed in the automotive industry as appropriate materials for sheet-forming operations associated with the industry. The application of Dual Phase steels for hydrogen purposes will be the main emphasis of this study. The steel melt is created in the converter using an oxygen top-blowing method, and in the secondary metallurgy stage, it receives an alloy treatment. The product is steel that has been killed by aluminum and has great tensile strength thanks to its composition of manganese, chromium, and silicon [19].

The following are their benefits: minimal yield strength, the ratio of yield strength to tensile strength is low (0.5), high rates of early strain hardening, excellent uniform elongation, high strain rate sensitivity (it absorbs more energy the faster it is crushed) [20], and it has good resilience to fatigue. DP steels are frequently used for automotive body panels, wheels, and bumpers as a result of these characteristics.[17] This thesis will extend the characteristics and features that make the dual phase steel adaptable in hydrogen application in the energy sector.

2.4.2 Complex phase steels

The microstructure and extremely small grain size of complex phase steels, which contain trace amounts of martensite, pearlite, and preserved austenite embedded in a ferrite-bainite matrix, contribute to their strength [21]. High grain refinement is accomplished through either postponed recrystallization or the

precipitation of micro alloying elements like Nb, Ti, or V. Both hot-rolled and cold-rolled [22]. Complex Phase steel are produced, and both can be hot-dipped galvanized to prevent corrosion [21]. The higher thickness ranges required to make structural-type parts are accessible in hot-rolled goods [21]. Except for the inclusion of a small amount of Nb, Ti, or V to provide a precipitation strengthening effect, CP steels have chemistry and microstructure that are comparable to Trip Steels [21][23]. The microstructure of the bainite complex phase demonstrates better strain hardening and strain capacity than the bainite structure alone [24]. For current and developing materials, the minimum tensile strength ranges from 780 to 1470 MPa with a total elongation of 5 to 30%.

The minimum yield strength of CP steels is higher when compared to dual-phase steels with equivalent tensile strengths of 800 MPa and above [21]. The yield strength to tensile strength ratio of CP steels is significantly higher than that of DP steels [21]. CP steels offer good work hardening capability at low strain, high wear resistance, high energy absorption, and high fatigue strength. With a heat treatment at 500–700 C, the yield point of hot-rolled CP steels can be increased by up to 100 MPa [25].

Spot welders for other steel types with lesser strengths can be used with the right adjustments. It is simple to weld CP steels to other common grades of steel or themselves. For present and developing strength, the minimum tensile strength classes range from 780 to 1470 MPa [26].

CP steels offer outstanding formability and are appropriate for stretch forming, roll forming, bending, and hole expansions due to their high uniform elongation and continuous yielding.

The excellent energy absorption capacity of CP steel makes it particularly suitable for the weight-saving production of cold-formed crash-relevant parts for automobiles. Applications for body structure, suspension, and chassis parts can be found in many automobiles [27].

Examples of CP steel applications and current production grades:

- CP 680/780 Frame rails, chassis components, cross members, B pillar reinforcements, and tunnel stiffeners
- CP 800/1000 Fender beams, suspension brackets, frame rail reinforcements, rocker panel supports, and bumper beams, side sills

Properties

- Tensile strengths that meet and exceed 800 MPa
- High ratio of yield to tensile strength
- Great for cold forming, bending, and hole expansion

- Strong bake-hardening qualities
- High durability and wear resistance
- High crash energy absorption
- Good weldability

2.4.3 TRIP steel

TRIP steels' microstructure allows for an exceptional fusion of strength and ductility [28]. As a result, they are appropriate for structural and reinforcing elements with intricate shapes. These steels have islands of hard residual austenite and carbide-free bainite scattered across a ductile ferritic matrix as its microstructure [29]. These steels have an exceptional balance of strength and ductility thanks to the transformation of austenite into martensite during plastic deformation (TRIP: Transformation Induced Plasticity effect). Due to their high capacity for strain hardening, these steels have outstanding drawability and a good aptitude for strain redistribution [28]. The tensile strength of TRIP steel improves significantly during the component manufacturing stages compared to its reference value for flat metal, both as a result of local stamping strains and the BH (Bake Hardening) effect during the painting process [30]. With a focus on crash behavior, these effects can be exploited to improve the part's design.

TRIP steels are especially well-suited for automobile structural and safety parts such crossmembers, longitudinal beams, B-pillar reinforcements, sills, and bumper reinforcements because of their excellent energy absorption capacity and fatigue strength [31].

2.4.4 Martensitic steel

Typically, a hard crystalline structure is referred to as martensitic. One of the three forms of stainless-steel alloy used in industry, martensitic steel is also a corrosion-resistant alloy [32].

The amount of carbon in this alloy, which determines its toughness and hardness, might be low or high. The amount of carbon in martensitic steel determines how tough and hard it is [32][33]. This steel alloy is tempered to further enhance its characteristics. Without tempering, martensitic steel becomes brittle and has a restricted range of uses [34].

Martensitic steel, a member of the stainless-steel family, is an alloy mostly made of chromium and is categorized as belonging to the ferromagnetic group. It comes in a variety of grades with various qualities to suit various industrial purposes [35]. Tempering, which alters the chemical makeup, and heat treatment, which makes it harder and more ductile, modify these qualities.

The following are examples of common uses for martensitic stainless steel: surgical instruments, gas turbines, cutting tools, springs, and ball bearings.

Martensitic steel's corrosion-resistant property makes it suitable for use in humid environments [36]. Additionally, it hardens when cooled in oil, water, or air. It is important to note that high-carbon martensitic steel is not recommended for welding [37]. Instead, a low-carbon alloy should be used for that purpose.

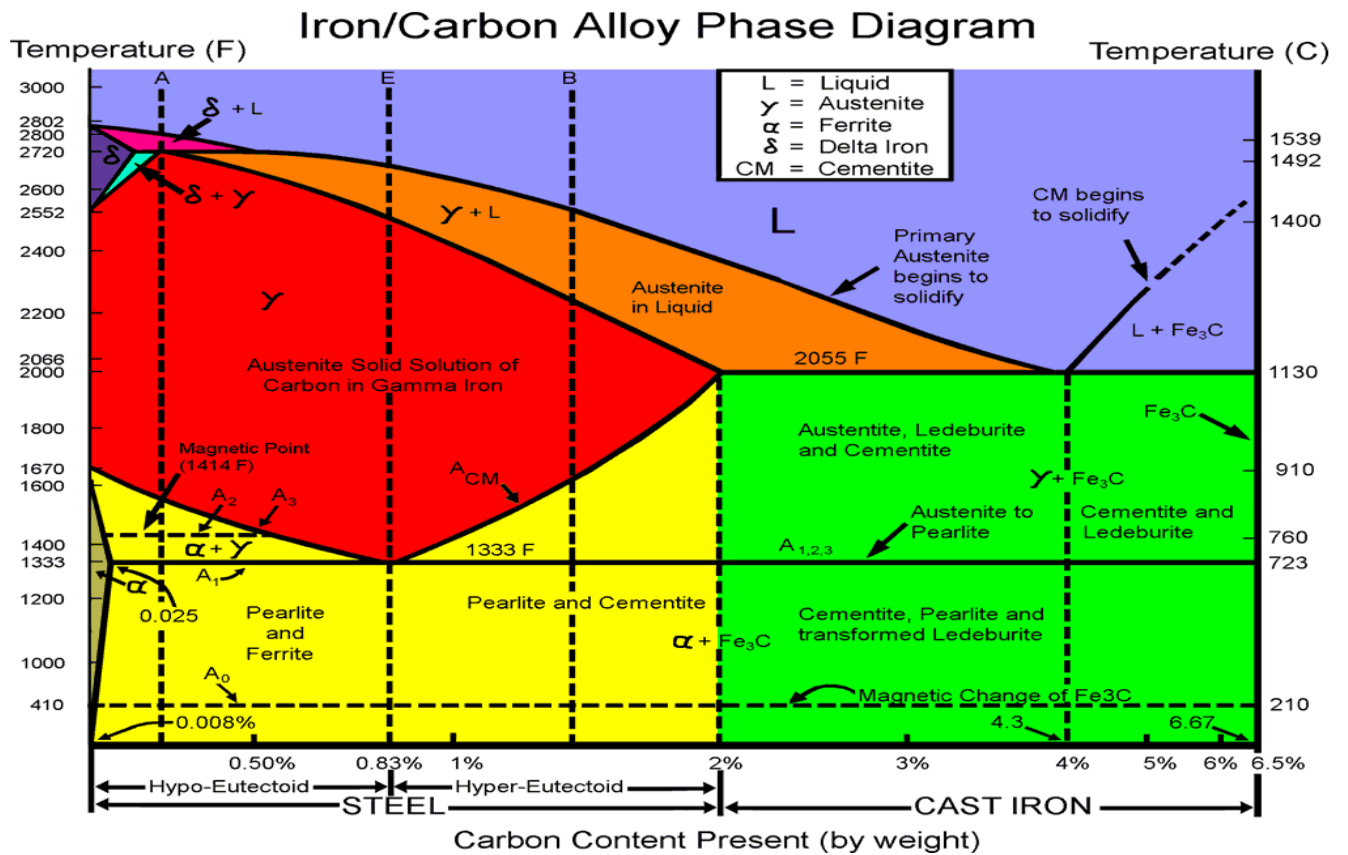


Figure 2: Iron/carbon alloy phase diagram [122]

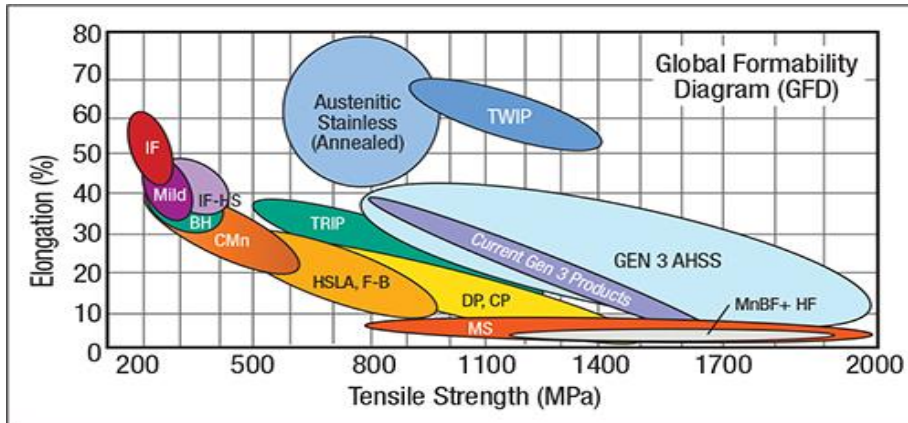
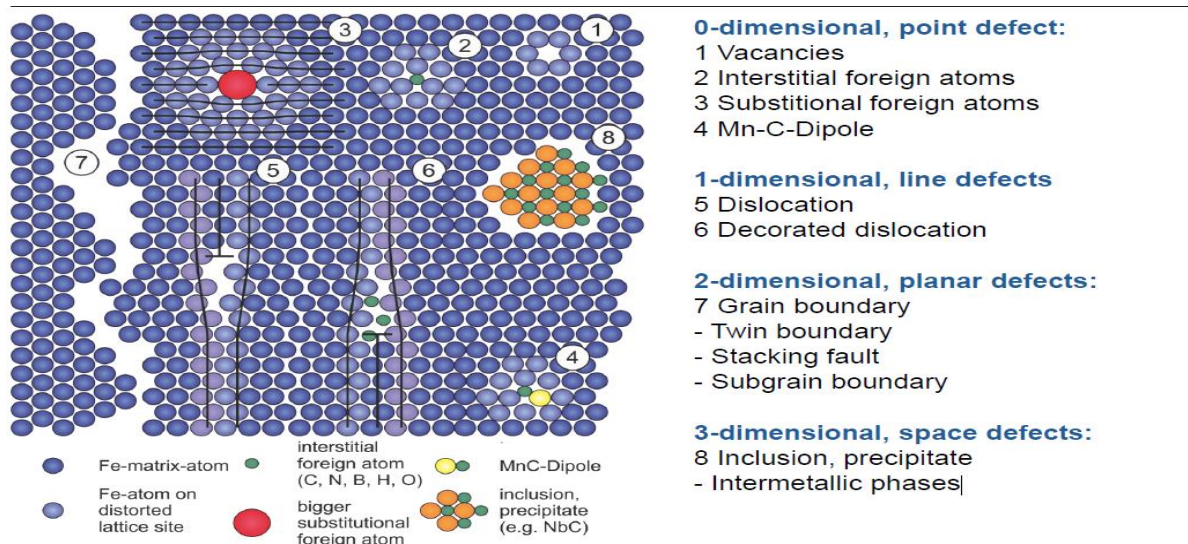


Figure 3: Strength against elongation graph depicting the range of properties for all known steels. [121]

2.5 Hydrogen Mechanisms

Due to its high mobility and tiny radius of 0.32 \AA ($1 \text{ \AA} = 10^{-10} \text{ m}$), hydrogen is very active in the metal lattice. Particularly when there are steel imperfections, born from steel manufacturing, the hydrogen atoms gather and interact with the matrix [38][39]. The uptake of hydrogen at the medium/steel interface, the adsorption of the hydrogen atoms, the trapping and diffusivity of hydrogen in steels are all important phases in the transfer of hydrogen from an ambient medium into solid steels [40][41]. Different factors, including the ambient medium, surface quality, temperature, and partial pressing, have an impact on each step's kinetics [40][42][43]. The next sections will go into the specifics of hydrogen behavior in steels.



Source: RWTH Aachen, IEHK

Figure 4: Presentation of all known defects in metals and their interaction with hydrogen atoms.

The production of pipes and the operation of hydrogen throughout the material's life are essential for the sector's use of hydrogen in the energy sector; nevertheless, for complete integration, the material must be properly characterized and developed [41].

2.6 Green Steel For Hydrogen Application

In green steel, hydrogen is added to the process during the melting of the steel when it is utilized as a reducing agent in the production of steel. The metallurgical process of green steel then produces $Ca(OH)_2$ in an extremely humid environment [44]. In the slag and water vapor, it can break down into CaO. Atomic hydrogen is introduced into the melt during the interaction between iron and water. Various oxides and hydroxides are generated on the surface of the sheet during the annealing, rolling, and cooling processes that are then used. Subsequently, in the pickling process, which comes before cold rolling or galvanizing, the sheet surfaces are treated with sulphuric acid or hydrochloric acid solution, which causes hydrogen uptake [45]. The steel sheets are cleaned in an alkaline electrolyte before galvanization. In direct current cycles, the steel coils are coupled as a cathode to remove the oil, emulsion, and contaminants from the band surfaces. Hydrogen is partially incorporated into the steel during cathodic cleaning [46]. An atmosphere made up of a mixture of nitrogen and hydrogen gas is employed during the hot-dip galvanizing process. An annealing process was conducted before the Zn-bath to create the desired microstructure and lessen the development of iron-oxide on the surfaces [47], as a result, hydrogen uptake occurs. In contrast, when electro-galvanizing, hydrogen is absorbed on the Fe/Zn contact. Additionally, the subsequent galvanizing creates a Zn-layer that serves as a barrier to stop hydrogen from escaping [48].

2.7 Hydrogen Pipeline Operation In The Energy Sector

The interaction of hydrogen atoms with the walls of the pipelines during their operation could cause corrosion [49]. The steel material's walls may have an appropriate polymer covering to stop leaks and penetrations in their tracks. These coatings aid in preventing hydrogen atom absorption when the pipe materials have flaws [50]. The corrosion of the pipeline is influenced by variables including temperature and humidity [51]. The following provides favorable conditions for the hydrogen entry reactions.

In general, hydrogen intake happens not only during the steelmaking process from a variety of sources but also because of the operation of the pipes during hydrogen transport and distribution [48]. Most hydrogen sources are now known to exist, and numerous techniques are used to minimize hydrogen entry [52]. The primary restriction in this case is the material's direct hydrogen exposure during operation.

2.8 Hydrogen Absorption And Transport In Steels

2.8.1 Hydrogen absorption

The material is designed specifically to transport pure hydrogen inside the pipeline and also prevent leaks. The inner and outer interphases of the hydrogen and steel should be in thermodynamic equilibrium. Since hydrogen is abundant and rarely found uncombined, the outer layer's temperature and pressure should be ambient, which results in little hydrogen absorption. To control or limit hydrogen absorption from the gaseous phase into the metallic lattice, partial pressures in the inner walls, where pure (atomic) hydrogen is mostly transported in gaseous forms, should be restricted to pressures less than 90 bar [53]. Under high partial pressures, hydrogen adsorption occurs in this sequence: accumulation, dispersion, and absorption. Under little exposure to corrosive materials, the steel begins to corrode. Zinc coatings is preferred over iron coating when protecting the steel from cathodic corrosion, the major corrosive mechanisms in steels. In a nutshell, the process of hydrogen absorption in steel substrates entails several/some phases and is influenced by variables such as cathodic current density, solution type, solution composition, substrate surface condition, etc. Atomic hydrogen and molecular hydrogen were the two forms of hydrogen that were absorbed into the steel substrate. The rate of Hydrogen evolution reaction (HER) and hydrogen absorption reaction (HAR) regulates the absorption.

With a good absorptive condition, the transport of hydrogen through the lattice occurs quickly. In steels, interstitial diffusion or the movement of defects facilitates hydrogen transport [54]. An optimal hydrogen concentration must be reached for the creation of hydrogen-induced cracking (HIC) [55]. In the area where a crack may form, the dissolved hydrogen diffuses and leads to further deformation in the steel lattice. Thus, the understanding of hydrogen solubility and diffusivity in steel is essential in the characterization and design of material for hydrogen application in the energy sector [56][57].

2.8.2 Hydrogen' solubility and diffusivity in steels

Hydrogen's atom further dissociates to form proton and electron in the lattice structure of the material it finds itself, in this case, the dual-phase steel. The movement of these sub-atomic particles in the lattice leads to the distortion. The presence of hydrogen in the lattice structure of steel can be quantified by the solubility of hydrogen in steel [58]. This solubility in atomic fraction is mathematically quantified by Sievert's law.

$$C_H = \alpha * \exp\left(-\frac{\partial H}{T}\right) \sqrt{P_H}$$

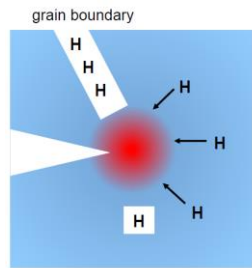
α = pre – coefficient

∂H = partial molar heat

T = Temperature

P_H = partial hydrogen pressure

Hydrogen can diffuse rapidly in steel, hydrogen concentration gradient is decisive in determining hydrogen diffusion. It provides details about the driving force to hydrogen atoms [59]. Fick's first law describes the diffusion flux density, which is defined as the number of hydrogen atoms that pass through a unit area in the unit of time, and it is proportional to the concentration gradient.



Source: RWTH Aachen, IEHK

Figure 5: A figure illustrating hydrogen diffusion towards region of higher hydrostatic stress.

$$J_D = -D * grad C = -D \left(\frac{\partial c}{\partial x} \right)$$

C = hydrogen concentration

D = hydrogen diffusion coefficient in crystallographic lattice of metallic solid, expressed in Arrhenius equation as

$$D = D_o * \exp\left(-\frac{Q}{RT}\right)$$

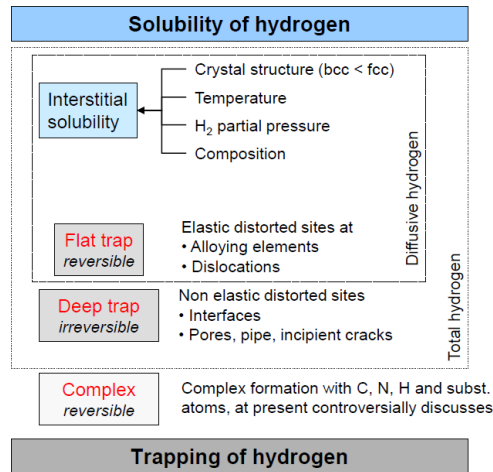
D_o = pre exponential factor

Q = activation energy

R = Universal gas constant = $3.814 \times 10^{-3} \text{ J} \cdot \text{mol}^{-1} \cdot \text{K}^{-1}$

T = Temperature

This parameter, D, depends on the material's microstructure hence it varies from material to material. Every has a unique make-up and microstructure. The ability of hydrogen to diffuse through materials depends on the material structure, the alloying element, and in some instances temperature and the stress state of the material. When there are defects in the material the diffusion within a material is interfered by the traps in the material. For that reason, the diffusion coefficient varies, that of dual-phase steel is between $2 - 2.7 \times 10^{-7} \text{ cm}^2 \text{ s}^{-1}$ [60][61].



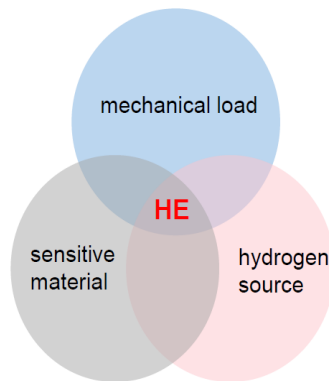
Source: RWTH, IEHK

Figure 6: A description of solubility of hydrogen in steels []

2.8.3 Hydrogen- induced defects and cracks in steels

The purpose of this thesis is to fully comprehend and predict the behavior of material under failure. All matters regarding embrittlement must be fully grasped, with the above-mentioned hydrogen-material interaction properties can provide a characteristic material design properties. The hydrogen embrittlement mechanism and its effects on dual-phase steels are going to be analysed in detail.

2.8.4 Hydrogen embrittlement



Source: W.H. Johnson, „On some remarkable changes produced in iron and steel by the action of hydrogen and acids“, Proceedings of the Royal Society of London, 23 (1875) 168 179

Figure 7: Hydrogen embrittlement summary []

The above illustration quantifies the explanation for HE; hydrogen embrittlement is a widely known phenomenon that occurs when certain metals become brittle and susceptible to cracking and failure under the influence of hydrogen interaction and mechanical load [46]. Hydrogen’s ‘unusual’ atomic size and

weight make it susceptible to penetrating and diffusing into the metal's structure. When in contact, hydrogen is absorbed by metals through various means such as surface reactions [62], electrochemical means, cathodic charging, or diffusion from a reactive corrosive surrounding environment, it then occupies interstitial sites within the crystal lattice and alters the chemical bonds consequently affecting the mechanical properties of the metal by reducing its ductility and toughness. This lattice distortion can weaken the material by affecting its dislocation movement, causing reduced ductility and increased susceptibility to fracture [63][64]. In the instance of in-built defects and residual stresses because of the production means, hydrogen diffuses to the deformed areas leading to localized high hydrogen.

Hydrogen's cohesive properties make it bond and this leads to lattice distortion and increased internal pressure. Any susceptible material under mechanical stresses will embrittle when exposed to hydrogen [65a], either irreversible or reversible. The reversible hydrogen embrittlement often leads to intergranular fracture [66]. Concerning the source of hydrogen, embrittlement can be considered Internal Hydrogen Assisted Cracking (IHAC) and Hydrogen Environment Assisted Cracking (HEAC). In IHAC atomic hydrogen diffuses into high-stress concentrated regions, these areas have high-stress areas which act as driving forces for the diffusion of atomic hydrogen [67]. When the material is loaded, Hydrogen-induced cracking occurs when the critical hydrogen concentration to crack is reached. In HEAC, the loss of mechanical properties occurs when there is hydrogen in the environment. After hydrogen's absorption into metals, several other embrittlement mechanisms are conceived, amongst these exist; Hydride Formation and fracture Theory (HFT), Hydrogen-Enhanced Decohesion (HEDE), Adsorption-Induced Dislocation Emission (AIDE), Hydrogen-Enhanced Localized Plasticity (HELP), Hydrogen-Enhanced Localized Plasticity (HELP) [68]. Hydrogen-Induced Cracking: The basis of the phenomenon is the subject matter of Hydrogen-Induced Cracking, it affects the formation and propagation of cracks in a material due to the presence of hydrogen [69]. Hydrogen-induced cracking and the amount of hydrogen embrittlement susceptibility increases with increasing temperature [70], also increased by the increase of hydrogen content in material [71]. Generally, hydrogen embrittlement susceptibility increases under the hydrogen-induced lattice defects formed due to the change in the hydrogen state, temperature, strain rate, and hydrogen content [72]. This is suggested by the reason that one of the atomic-level changes that occur in the substructure of pearlitic steels exhibits higher hydrogen embrittlement susceptibility and an enhancement of the formation of hydrogen-induced lattice defects [73][74].

Hydrogen can promote crack initiation and propagation through Hydrogen-enhanced decohesion (HEDE). Hydrogen atoms can weaken the atomic bonds at grain boundaries or interfaces, reducing the material's resistance to crack initiation and promoting intergranular fracture [75]. In some cases, the presence of hydrogen can result in a phenomenon known as hydrogen-enhanced localized plasticity (HELP). HELP involves the formation of localized plastic deformation zones, such as shear bands or deformation twins,

which can accommodate a significant amount of plastic strain. The presence of hydrogen facilitates the nucleation and propagation of these deformation features, leading to localized plasticity and strain concentration. Hydrogen has been shown to interact with dislocations and to be transported by mobile dislocations. In addition to enhancing hydrogen transportation and the contribution this makes to hydrogen embrittlement, the presence of hydrogen either on the dislocation core, in the dislocation stress field or on the slip plane ahead of the dislocation serves to enhance the velocity of the dislocations. The effect of this enhancement is that dislocation processes and interaction with other obstacles occur at lower stress in the presence of hydrogen than in the absence. Recent progress has been made in establishing the link between hydrogen-enhanced plasticity and fracture [76]. However, excessive strain localization can promote crack initiation and contribute to embrittlement. Hydrogen-enhanced dislocation (HED) activity causes hydrogen to interact with dislocations, affecting their mobility and interaction with other dislocations. This can lead to increased dislocation pile-up, strain localization, and the formation of microcracks. The damage evolution process in martensite-ferrite dual-phase steels can be generally understood in terms of three basic regimes, namely, damage incubation, damage nucleation, and damage growth. Hydrogen charging strongly affects all of them. Hydrogen decreases the critical strain for the decohesion in martensite regions, promotes ferrite/martensite cracking and ferrite/martensite boundary sliding, and cracks of the ferrite grains in dual-phase steels, and causes macroscopic hydrogen embrittlement. [77]

2.8.5 The mechanism of Hydrogen-induced Cracking

The whole hydrogen embrittlement concept in common knowledge is the interaction between a material, for this thesis, dual-phase steel, a hydrogen source and it is propagated by stress.

The materials that are used to transport hydrogen are examined to know its susceptibility to embrittlement. The embrittlement mechanism varies by material type, hydrogen concentrations, loading conditions, and environmental factors. The susceptibility of quenched and tempered martensitic steels to hydrogen embrittlement occurs at yield strengths greater than 1035 MPa. The dual-phase, ferrite plus martensite, steels that are first finding applications have a yield stress of about 345 MPa (50 ksi) and a tensile strength of about 655 MPa (95 ksi) [17]. Thus, from a consideration of strength alone, these dual-phase steels would not be expected to be susceptible to hydrogen embrittlement. However, these dual-phase steels have a structure consisting of 15 to 20 vol. pct high carbon martensite (0.5 to 0.6 pct C) with a tensile strength above 2070 MPa (300 ksi), in a ductile ferrite matrix [17]. Two dual-phase steels with similar tensile properties but different chemical compositions and thermal histories were experimented to observe the influence of hydrogen on the ductility of the material. One of the dual-phase steels experimented had a vanadium and was air-cooled from the inter-critical at approximately +7°C region and the other had a lower

alloy steel that was water-quenched from an inter-critical temperature and tempered at approximately 260 °C for a few minutes. The composition of this steel is shown

COMPOSITION IN Weight Pct of Alloys Investigated					
	C	Mn	Si	V	P
Alloy A*	0.11	1.48	0.55	0.09	----
Alloy B ~	0.08	0.41	0.06	---	0.04
* Supplied by Jones and Laughlin Steel Co.					
~Supplied by Inland Steel Co.					

Table 1: Composition in Weighted percentages of alloyed investigated [17]

Steels were presented in 0.8 mm thick sheets, and double-notched samples were used in addition to typical tensile specimens. The entire testing was carried out in an Instron tensile machine with a crosshead rate of 0.042 mm/s (0.1 in./min) [79]. The experiment confirmed that indeed dual-phase steels are susceptible to hydrogen embrittlement, but this susceptibility is different from quenched and tempered martensitic steels because dual-phase steels do not contain boundaries between prior austenite grains. Fracture in hydrogen charged dual phase steels appears to involve cleavage of both the martensite and ferrite phases and requires the expenditure of a large amount of work. Stress concentrations arising from the different rates of strain hardening of the ferrite and martensite may be required for crack initiation [80].

In summary, hydrogen embrittlement involves multiple mechanisms, including hydrogen absorption, hydrogen-induced cracking, and hydrogen-enhanced localized plasticity. These mechanisms can collectively weaken the material, reduce its ductility, and lead to sudden brittle fracture. A precise understanding of these mechanisms is essential for developing strategies to mitigate hydrogen embrittlement and designing materials that are more resistant to hydrogen-related degradation.



Figure 8: Hydrogen embrittlement reaction procedure [78]

2.9 Material Characterization Techniques for DP Steel

Dual-phase steel consists of two distinct phases: a soft ferrite phase and a hard martensite phase. The mechanisms of hydrogen absorption, diffusion, and trapping, and their influence on the dual-phase steel properties are thoroughly explained and understood by these methodologies. These cutting-edge characterization techniques examine the impact of hydrogen on the solid material (dual phase) in detail. The detailed characterization of materials at the nanoscale is made possible by advanced characterization methods used to study hydrogen-material interactions, such as transmission electron microscopy (TEM) and scanning transmission electron microscopy (STEM) [82]. In nanotechnology, electron microscopes have enabled the study of submicron-sized objects, even down to individual atoms. For characterizing materials in many industries, electron microscopy has become increasingly important. These methods can reveal microstructural modifications brought on by hydrogen during its interactions between dislocations, crack development, and grain boundary and the resultant effects. The increased picture resolution of electron microscopy over light microscopy is its principal benefit. Modern transmission electron microscopes can examine the location and chemical composition of individual atoms [83], though as we will see in this thesis, the resolution of data is dependent on the technique for electron microscopy that is used and the conditions under which the microscope is operated. A very high magnification range is available with electron microscopes, typically between 2000 and 1 million times for TEM and 10^{500000} times for SEM. This makes it possible to characterize microstructures at a variety of length scales, from micro to nano, during an imaging session. Which is crucial for the material characterization and design in this research. Moreover, the fact that electrons interact aggressively with atoms due to their negative charge is a significant benefit of using them instead of light.

The Atom Probe Tomograph (APT) provides a three-dimensional atomic-scale analysis of materials that pinpoints hydrogen atom distribution and location as well as their clustering behavior, segregation, and effects on the local composition and microstructure [84]. Nuclear Magnetic Resonance (NMR) is used to study hydrogen's behavior at the atomic scale in bonds, traps, and during diffusion. It sheds light on how hydrogen interacts with lattice flaws such as grain boundaries, vacancies, and dislocations [85]

These cutting-edge characterization methods offer important insights into the fundamental mechanisms and processes regulating hydrogen-material interactions. They support the creation of materials that are more resilient to hydrogen embrittlement, have greater hydrogen storage capacity, and function better in applications involving hydrogen in the energy industry and other industries. The perceivable description of the dual-phase steel is observed by optical microscopy, and it provides a macroscopic view of the ferrite and martensite phase and allows for the measurement of phase volume fraction and grain sizes.

When the engineering components' functionality is reduced, structural failure occurs. In general, excessive (elastic or inelastic) deformation, fracture, and wear are the three basic causes of a component becoming dysfunctional. For the characterization methods, the material's response to load and shear should be fully investigated and understood. Excessive elastic deformation can happen under loading conditions of stable equilibrium, and brittle fracture. Elastic deformation is governed by the elastic properties of the material, such as elastic modulus. Inelastic deformation can happen under loading conditions that are conducive to fatigue (a process involving alternating stresses (or strains) that cause crack initiation from stress raisers or defects in the material followed by crack growth), ductile fracture, and other failure modes. Mechanical testing techniques, such as tensile testing, hardness testing, and impact testing, are essential for characterizing the mechanical properties of the steel. These tests provide information about the strength, ductility, toughness, and deformation behavior of the material under different loading conditions [17].

In particular, in circumstances of slow and persistent deformation, the slow strain rate test (SSRT) is a mechanical testing technique used to assess the susceptibility of materials to environmentally assisted cracking [86]. It is frequently used to evaluate the susceptibility of metallic materials to hydrogen embrittlement. The SSRT entails subjecting a specimen to a corrosive environment at a continuous strain rate, generally in the presence of hydrogen.

In a continuously annealed dual-phase sheet steel, the ferrite and martensite phases were carried out in the as-received state both in their pre-deformation state and after. The main conclusions are: In the as-received condition, the hardness and strength of ferrite within specific ferrite grains are not spatially uniform; the ferrite close to the ferrite/martensite contact is harder and stronger than the ferrite inside the grain. The

ferrite near the ferrite/martensite interface softens while hardening in the interior of the dual-phase steel during subsequent tensile deformation; the inhomogeneous reaction lasts at least up to 7% of the dual-phase steel's overall plastic strain [17]. Around 395 MPa is when ferrite starts to yield under compression. The hardening response that follows yielding in ferrite in compression is orientation-dependent and is greatest for the [0 0 1] loading axis. The beginning of yielding in ferrite in compression begins at about 395 MPa. Micropillar compression tests show that martensite yields at 1 GPa, hardens quickly to 1.5 GPa, and then hardens more slowly to 2.3–2.5 GPa [87]. The initial yielding of the dual-phase steel and the beginning of the ferrite's plastic deformation are closely correlated. However, it is crucially demonstrated that the beginning of the plastic flow and the hardening of martensite occurs well before the dual-phase steel reaches its maximum tensile strength [88]. These microscale experiments offer crucial data and insights into the deformation properties of the individual phases, which can then be used as valuable input into computations based on microstructure to forecast the flow behavior of these multiphase alloys under various stress states.

2.10 Hydrogen charging methods

Hydrogen can be introduced into the dual-phase steel through electrochemical methods to give a proper understanding of its effects on the material. These methods allow for a controlled and precise introduction of hydrogen into the material to make it mimic the hydrogen absorption that occurs in real-world environments. For the case of this thesis electrochemical methods of hydrogen charging were used. Here is some other electrochemical charging in dual-phase steel: Cathodic Charging; Hydrogen Permeation cell; electrochemical hydrogen charging; and electrochemical cell with hydrogen gas evolution. These electrochemical methods offer precise control over the introduction of hydrogen into the dual-phase steel, allowing to study of the effects of hydrogen charging on material properties, such as mechanical behavior, microstructure, and hydrogen embrittlement susceptibility [89][90]. It is important to carefully design and conduct these experiments, considering factors like charging conditions, electrolyte composition, temperature, and the specific research objectives. Electrochemical Impedance Spectroscopy (EIS), and other electrochemical techniques are used to highlight their applications in evaluating the corrosion behavior and mechanical integrity of materials subjected to hydrogen charging. The parameters influencing the hydrogen charging process and their impact on material performance are analyzed: the charging current density, state of the charge, temperature, presence of oxygen, and the charging method. Through thermal desorption spectroscopy measurement and theoretical analysis, it was revealed that electrochemical (E-) charging induces steep gradient of H concentration near the surface while H was homogeneously distributed after gaseous (G-) charging.

The charging current density is a significant factor that affects hydrogen absorption in dual-phase steel, according to the search findings. The current study looked at the mechanical characteristics of prestrained

high-strength steels about cathodic hydrogen-charging current density. Three different current densities were used to cathodically charge the samples: $0.8\text{mA}/\text{cm}^2$, $8.3\text{mA}/\text{cm}^2$, and $62.5\text{mA}/\text{cm}^2$ [91]. The charge current density is the major deciding factor in cathodic hydrogen charging. Current density and the presence of oxygen are the most important variables affecting the electrochemical hydrogen charging process of carbon and low alloy steel. Therefore, it can be said that the dual-phase steel's ability to absorb hydrogen is significantly influenced by the charging current density [92].

2.11 Alloying design for Hydrogen Compatibility

To increase the resistivity of a dual-phase steel material in hydrogen application in the energy sector to increase its compatibility with hydrogen application, there can be the incorporation of specific alloying elements to enhance the material's resistance to hydrogen embrittlement [93]. To improve hydrogen's compatibility in dual-phase steel the material can be alloyed with one of the following strategies: Alloying with Precipitation-Strengthening Elements, Alloying with Hydrogen Trapping Elements, Alloying with Grain Refiners, Alloying with Austenite Stabilizers, and Alloying with Hydrogen Permeation Barrier Layers [94]. To obtain the appropriate combination of mechanical characteristics, hydrogen compatibility, and processability, it is crucial to highlight that the choice of alloying elements and their concentrations should be carefully tuned [93][94]. A stable austenitic stainless steel with a Fe-Cr-Ni composition can have a higher strength-ductility balance thanks to the alloying element hydrogen [93]. It has been discovered that adding alloying elements like niobium, vanadium, and titanium increases the resistance of dual-phase steel to hydrogen embrittlement [95] [96]. Carbides may effectively trap hydrogen, removing the harmful mobile hydrogen from the microstructure, which is generally thought to be advantageous in enhancing the hydrogen embrittlement resistance of steels [93]. Comparing tempered martensite structures to bainitic structures, it has been discovered that the resistance is improved by 10–20%. The best resistance to hydrogen embrittlement was discovered in dual-phase steels with a tempered martensite matrix and 20% bainite [97]. The hydrogen-induced cracking and sulphide stress cracking behaviours of A516-65 steels in sour environments be improved by carbon and molybdenum. alloying substances [94].

The alloying design should also take other aspects like cost, manufacturability, and microstructural stability into account. These alloying techniques enable the safe and dependable use of dual-phase steel in hydrogen applications in the energy industry by tailoring it to have higher resistance to hydrogen embrittlement. The material can also be coated to reduce the HE effects on the material.

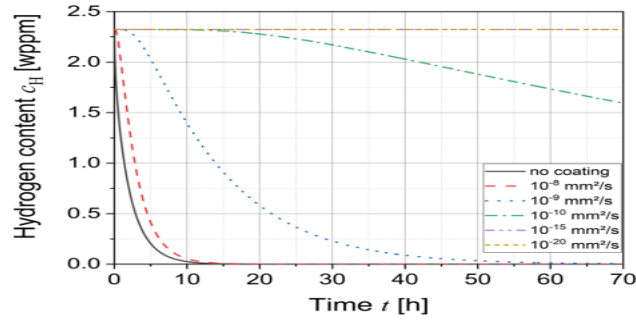


Figure 9: Hydrogen absorption on DP steels with and without coating [124]

2.12 Phase Equilibrium of DP Steel during interaction with Hydrogen

The distribution and stability of the various phases inside the material when exposed to a hydrogen environment is referred to as the phase equilibrium of dual-phase steel materials in the presence of hydrogen. When hydrogen is present, it can have an impact on the phase composition and properties of the ferrite and martensite phases that make up dual-phase steel. Generic Fe-C lab-cast alloys made of a single phase, such as ferrite, bainite, pearlite, or martensite, have been used to study the interaction between hydrogen and the microstructure of steel [98]. Since carbides may effectively trap hydrogen, removing the harmful mobile hydrogen from the microstructure, they are generally thought to be advantageous in strengthening the hydrogen embrittlement resistance of steels [98]. Niobium, vanadium, and titanium were used as microalloying elements in dual-phase steel that was evaluated for hydrogen embrittlement and found to have increased resistance [95]. Comparing tempered martensite structures to bainitic structures, it has been discovered that the resistance is improved by 10–20%. The best resistance to hydrogen embrittlement was discovered in dual-phase steels with a tempered martensite matrix and 20% bainite [99].

The equilibrium between the ferrite and martensite phases may change when hydrogen interacts with dual-phase steel. Due to its open lattice structure, ferrite has poor solubility yet a fast hydrogen diffusion rate [100]. It has been discovered that ferrite-austenite contacts serve as hydrogen-trapping sites. Compared to ferrite, austenite has a substantially higher solubility of hydrogen and a much lower diffusivity of hydrogen [101]. Due to the existence of residual austenite, martensitic steels have a higher hydrogen solubility. Ferrite-martensite dual-phase steels get their ductility from the continuous ferrite phase and their strength from the martensite phase. The hydrogen can interact with the crystal lattice and diffuse into the material, changing the phase distribution and perhaps impacting the material's mechanical properties. Several variables, including hydrogen concentration, temperature, applied stress, and charging current density affect the phase equilibrium.

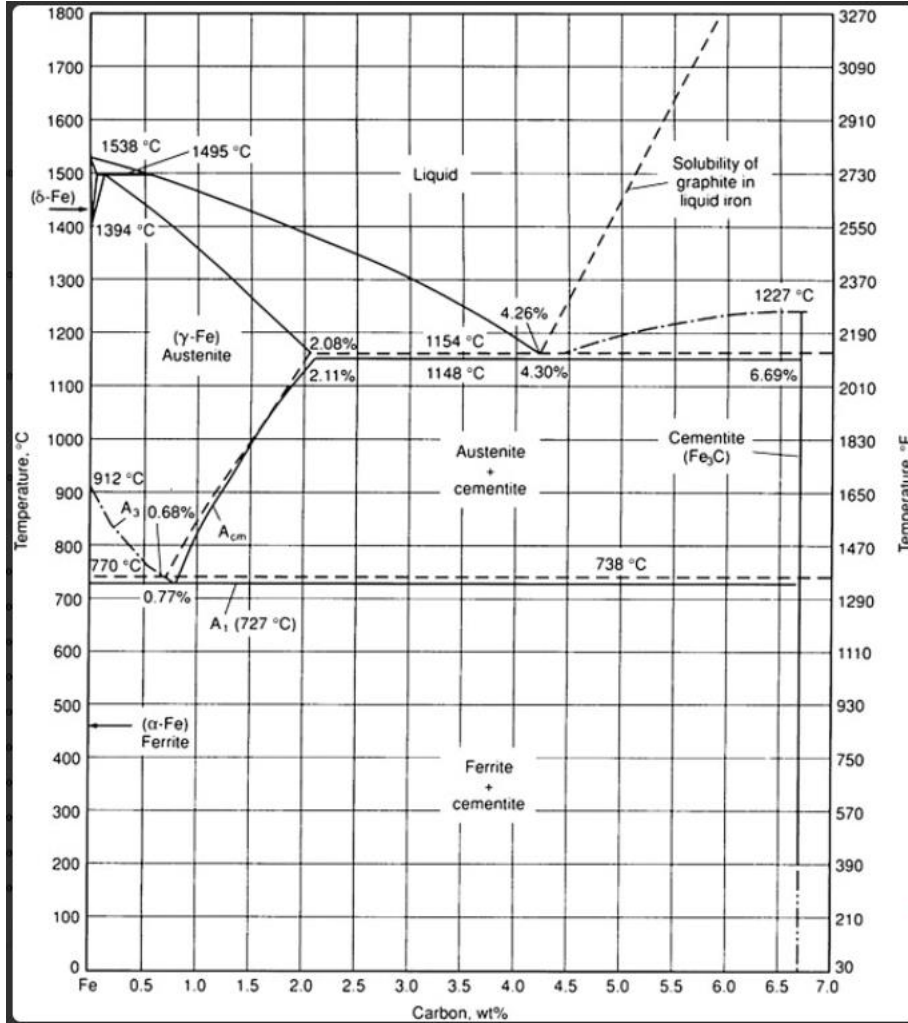


Figure 10: Effect of temperature, charging current density and phase composition [121]

Dual-phase (DP) steels exhibit stress-strain behavior that is distinctively different from high-strength low-alloy (HSLA) steels [102]. Due to the strain incompatibility of the martensite and ferrite phases and stress concentration caused by the difference in the elastic modulus of the two phases, DP steels are prone to microcrack nucleation [103]. For martensite, when the stress is greater than 550 MPa, the dislocation density increases rapidly and the tensile strength of DP steel increases [104].

2.13 Importance of alloying methods in Hydrogen application

Alloying designs play a crucial role in improving hydrogen compatibility in dual-phase steel. By carefully selecting and incorporating specific alloying elements, the material's resistance to hydrogen embrittlement can be enhanced. Some common alloying strategies used to improve hydrogen compatibility in dual-phase steel: Alloying with Precipitation-Strengthening Elements: The strength and stability of the dual-phase steel

can be increased by using precipitation-strengthening metals including chromium (Cr), molybdenum (Mo), and vanadium (V) [93]. These alloying components create intermetallic precipitates such as carbides, nitrides, or precipitates that serve as barriers to hydrogen diffusion and lessen the susceptibility to hydrogen embrittlement. Alloying with Hydrogen Trapping Elements [105]: It is possible to improve the material's capacity to hold hydrogen inside the microstructure by using hydrogen-sealing elements like titanium (Ti), niobium (Nb), or zirconium (Zr). Due to their strong hydrogen affinities, these elements can create stable hydrides that can efficiently trap and restrict the mobility of hydrogen atoms, hence lowering the possibility of embrittlement [93][106]. Alloying with Grain Refiners: In dual-phase steel, the addition of grain refining elements like aluminum (Al) or niobium (Nb) encourages the development of fine-grained microstructures [107]. The higher grain border area that fine grains provide can be an efficient hydrogen trapping location. Additionally, grain refining prevents hydrogen-induced cracks from spreading, strengthening the material's resistance to embrittlement [108]. Alloying with Austenite Stabilizers: The addition of substances like nickel (Ni), manganese (Mn), or copper (Cu) that help to maintain the austenite phase can increase the resistance of dual-phase steel against hydrogen embrittlement [109]. Since austenite is more soluble in hydrogen than other phases, it can hold more hydrogen without becoming embrittled. Alloying with Hydrogen Permeation Barrier Layers: The hydrogen ingress can be reduced by covering the surface of the dual-phase steel with a layer that prevents hydrogen permeability. To avoid or drastically minimize hydrogen absorption into the material, barrier layers made of materials like palladium (Pd) or certain alloys with low hydrogen solubility are utilized [110].

The importance of emphasizing that the choice of alloying elements and their concentrations should be carefully adjusted to achieve the desired mix of mechanical properties, hydrogen compatibility, and processability cannot be overstated. Other factors including cost, manufacturability, and microstructural stability should be considered in the alloying design as well.

By employing these alloying strategies, dual-phase steel can be tailored to have improved resistance to hydrogen embrittlement, enabling its safe and reliable use in hydrogen applications in the energy sector. The literature review then delves into alloy design strategies for enhancing hydrogen compatibility. The influence of alloying elements, including transition metals and interstitial elements, on hydrogen absorption and embrittlement is reviewed. The mechanisms by which these elements mitigate or exacerbate hydrogen embrittlement are discussed, providing insights into the design of alloys with improved resistance to hydrogen-induced degradation.

One possible effect of hydrogen on the phase equilibrium is the preferential absorption of hydrogen by specific phases. For example, hydrogen may have a higher solubility in ferrite compared to martensite, leading to an increased hydrogen concentration in the ferrite phase. This preferential absorption can result in changes in the phase volume fractions and microstructural properties of the dual-phase steel [111] [112].

Moreover, hydrogen can induce phase transformations in dual-phase steel. It can promote the formation of additional phases, such as the transformation of austenite to ferrite or martensite. The presence of hydrogen can also lead to the formation of hydrides within the material [113], altering the phase distribution and introducing new phases [114].

The phase equilibrium in the presence of hydrogen is critical to understanding the material's behavior and susceptibility to hydrogen embrittlement. It is important to investigate how hydrogen interacts with the different phases, the kinetics of phase transformations, and the influence of hydrogen on the mechanical properties of the material.

Experimental techniques such as microscopy, diffraction methods (e.g., XRD, TEM), and thermal analysis can be employed to analyze the phase equilibrium of dual-phase steel in the presence of hydrogen [115]. These techniques provide insights into the changes in phase composition, crystal structure, and microstructure caused by hydrogen interactions, aiding in the understanding and design of hydrogen-compatible dual-phase steel materials.

Phase diagrams and computational modeling are valuable tools used to predict the phase stability and hydrogen solubility in alloys. They provide insights into the thermodynamic and kinetic behavior of hydrogen in various alloy systems. Here's a discussion on their use in predicting the phase stability of hydrogen solubility in alloys: Phase diagrams depict in the context of hydrogen solubility in alloys the information about where hydrogen can dissolve and the solubility limit with details about the temperature causing that, composition, and phase(s) present in a material system [116][117][118]. They are commonly used to understand the equilibrium phases and their stability under different conditions. In the context of hydrogen solubility in alloys, phase diagrams can provide information on the phase regions where hydrogen can dissolve and the associated solubility limits.

The examination phase diagrams can identify the alloy compositions and temperature ranges that favor the dissolution of hydrogen into solid solution phases or the formation of hydrides. Phase diagrams also help in determining the conditions under which phase transformations may occur due to hydrogen absorption or desorption [119]. They provide a macroscopic view of the material system and serve as a guide for designing alloys with desired hydrogen solubility characteristics.

Computational Modeling: Computational modeling, particularly using methods like density functional theory (DFT) and Monte Carlo simulations, allows for atomistic-level understanding of hydrogen interactions with alloys. These models can provide insights into the thermodynamics and kinetics of hydrogen solubility, diffusion, and trapping mechanisms in different alloy structures. Computational modeling enables researchers to predict the energetics of hydrogen incorporation in various lattice sites, evaluate the binding energies between hydrogen and alloying elements, and estimate the equilibrium hydrogen solubility in alloys. Additionally, these models can simulate the effects of temperature, pressure, and alloy composition on hydrogen behavior, aiding in the prediction of phase stability and hydrogen-induced phase transformations [120].

Furthermore, computational modeling can facilitate the exploration of vast alloy composition and structure spaces, guiding the design of new materials with tailored hydrogen solubility properties. It can also help in understanding the atomic-scale mechanisms behind hydrogen embrittlement phenomena and assist in the development of mitigation strategies.

By combining experimental data with phase diagrams and computational modeling, a comprehensive understanding of the phase stability and hydrogen solubility in alloys can be gained. This integrated approach allows for the prediction and optimization of alloy compositions, processing conditions, and microstructures to achieve desired hydrogen-related properties, ensuring the development of alloys suitable for hydrogen applications in the energy sector.

Phase transformations, such as martensitic transformation and precipitation, play a significant role in determining the susceptibility of materials to hydrogen embrittlement. Understanding the impact of these transformations is crucial for alloy design and materials selection in hydrogen-related applications. Here is a discussion on their influence: Martensitic transformation involves a diffusionless, displacive structural change in materials, leading to the formation of a new phase with a different crystal structure. This transformation is often accompanied by a significant change in the material's mechanical properties. In the context of hydrogen embrittlement, martensitic transformation can have both positive and negative effects.

The formation of martensite can offer increased resistance to hydrogen embrittlement. The transformed martensitic phase often exhibits higher strength and toughness compared to the original phase, thereby improving the material's resistance to hydrogen-induced cracking and localized plasticity. The formation of a hardened martensitic structure can also impede hydrogen diffusion and reduce hydrogen uptake into the material, lowering the overall hydrogen concentration. However, martensitic transformation can also introduce new interfaces, such as grain boundaries and phase boundaries, which can act as preferential sites for hydrogen trapping and embrittlement. These interfaces may provide localized regions of high stress and

hydrogen concentration, leading to hydrogen-induced cracking and degradation of mechanical properties. The extent of embrittlement depends on factors such as the specific alloy composition, hydrogen concentration, and loading conditions.

Precipitation refers to the formation of secondary phases within a material due to the diffusion and clustering of solute atoms. These precipitates can significantly influence the material's microstructure and mechanical properties, including its susceptibility to hydrogen embrittlement. The presence of precipitates can enhance the resistance of materials to hydrogen embrittlement. Precipitates act as trapping sites for hydrogen, reducing its availability for diffusion and minimizing its detrimental effects on the material's mechanical properties. Precipitates can also act as barriers to hydrogen diffusion, hindering its movement within the material and decreasing the likelihood of embrittlement. However, the presence of certain precipitates can also increase the susceptibility to hydrogen embrittlement. Some precipitates may have a high affinity for hydrogen, leading to their preferential occupation and subsequent embrittlement of the material. Moreover, the interaction between hydrogen and precipitates can induce changes in their size, distribution, and stability, further influencing the embrittlement behavior.

By studying the influence of phase transformations, such as martensitic transformation and precipitation, on hydrogen embrittlement susceptibility, valuable insights can be gained for alloy design and materials selection. Experimental techniques, such as microscopy, diffraction methods, and mechanical testing, combined with computational modeling, can be employed to investigate the microstructural changes, hydrogen distribution, and mechanical response associated with these phase transformations. These findings aid in the development of hydrogen-resistant alloys with optimized microstructures and enhanced resistance to embrittlement in hydrogen environments.

2.14 Hydrogen Storage and Transportation Mechanisms and Technologies

In the energy sector, there are various materials and technologies used for hydrogen storage and transportation. These include: Hydrogen can be stored in high-pressure cylinders made of durable and lightweight materials like steel or carbon fiber-reinforced composites. Transporting large amounts of hydrogen is possible with tube trailers, which are long cylinders that can hold several compressed gas cylinders. At very low temperatures (-253°C), hydrogen can be kept as a liquid. Cryogenic tanks are well-insulated storage spaces that keep the temperature low enough to keep hydrogen liquid. Metal hydrides are compounding certain metals, like magnesium or titanium, which can be created with hydrogen. These substances offer a secure and reversible form of hydrogen storage since they can collect and release hydrogen.

As hydrogen transporters, chemicals like methanol (CH_3OH) and ammonia (NH_3) can be used. They are simple to transport and store, and when necessary, hydrogen may be released chemically.

Some organic molecules can have hydrogen chemically linked to them, serving as carriers. Through a catalytic process, these substances can be transferred and then released hydrogen. Like how natural gas is stored underground, hydrogen can be kept in salt caverns. Large-scale, safe storage is possible in salt deposits. In some areas, hydrogen is transported using pipelines that are specifically intended for that purpose. These pipelines have been built with hydrogen-compatible materials and are properly secured.

Materials like metal-organic frameworks (MOFs) and porous carbon materials can store hydrogen in their structure. These materials have high surface areas and can adsorb hydrogen molecules, providing a potential solution for efficient hydrogen storage.

It is important to note that each storage and transportation method has its advantages and challenges in terms of efficiency, safety, infrastructure requirements, and cost. The choice of materials and technologies depends on factors such as the scale of storage, transportation distance, required storage duration, and specific application requirements. Ongoing research and development aim to improve the efficiency and viability of these storage and transportation methods for widespread adoption of hydrogen as an energy carrier.

3 MATERIALS AND EXPERIMENTAL METHODS

3.1 Examined Material and its composition.

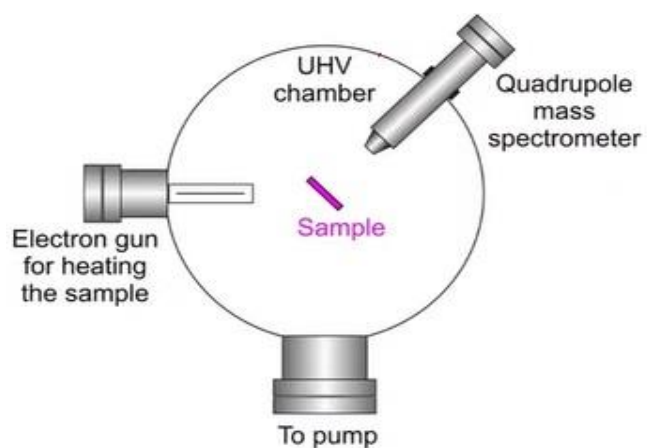
To this thesis, dual-phase steel DP980 steel was investigated. From the tensile strength and microstructure of the material the name DP980 was made, the material has a tensile strength of 980 MPa. It is an industry-produced steel. As mentioned in the literature review, detailed information about the material is investigated by the advanced characterization method. The chemical composition of the material was measured by electron microscopy. Thermal Desorption Spectroscopy, which will be explained in detail, was used to analyze the hydrogen concentration in the dual-phase steel, DP980, at several concentrations and currents.

3.2 Hydrogen charging and analysis

The intentional introduction or absorption of hydrogen in a material, dual-phase steel, is widely known as hydrogen charging. This process was carried out to study the effects hydrogen has on the mechanical properties of dual-phase steel. Hydrogen can be introduced into a DP steel by electrochemical hydrogen charging, gaseous hydrogen charging, and by hydrogen permeation test. For this thesis, the hydrogen permeation approach was used.

3.2.1 Thermal Desorption Spectroscopy

DP steel's metallic materials can have their hydrogen concentration measured via Thermal Desorption Spectroscopy (TDS). In TDS, a sample is heated to liberate the hydrogen, which is then found and analyzed. Hydrogen concentration measurements can be more precise when samples are cooled during TDS tests. TDS has been used to predict hydrogen bulk diffusion in dual-phase steels as well as to examine hydrogen uptake and desorption in high-strength carbon steels. For this thesis, heating rate applied was 0.3 K/s. To desorb diffusible hydrogen from the sample surface, all samples were heated to 1000 K. An extra thermocouple was installed adjacent to each sample in the infrared furnace to measure the sample's real temperature. The furnace was cooled to room temperature following each measurement. Incorporating the obtained TDS spectrum allowed for the determination of the hydrogen concentration.



Source: M.Meyer et al Phys. Chem. Chem. Phys., 10,4932 (2008)

Figure 11: Phenomenon behind TDS experiment []

The TDS peak temperatures were determined in a rather straightforward manner without fitting of Gaussian curves.

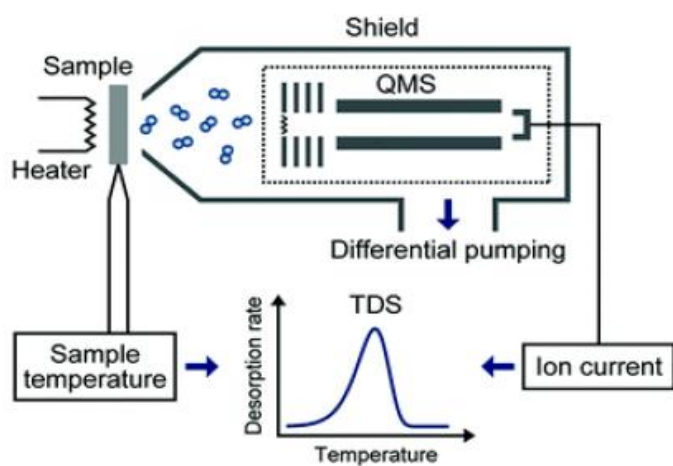


Figure 12: TDS summary

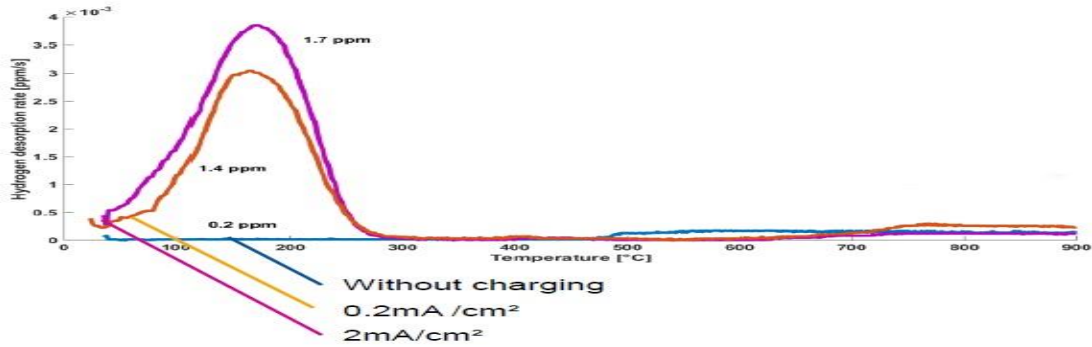


Figure 13: A graph of TDS showing the effect of charging on hydrogen absorption rate []

3.3 Thermal Desorption Spectroscopy measurement

Title: The varying conditions of pressure, current density, and temperature in a tabular form for all 22 data set.

TEST	PRESSURE (MPa)	CURRENT DENSITY	DURATION	TEMPERATURE(K)
SAMPLE TEST 1	0 MPa	0 mA/cm ²	1 hour	0 K
SAMPLE TEST 2	0 MPa	0 mA/cm ²	1 hour	0 K
SAMPLE TEST 3	0 MPa	0 mA/cm ²	1 hour	0 K
SAMPLE TEST 4	0 MPa	0.02 mA/cm ²	1 hour	0-1000K
SAMPLE TEST 5	0 MPa	0.02 mA/cm ²	1 hour	0-1000K
SAMPLE TEST 6	0 MPa	0.02 mA/cm ²	1 hour	0-1000K
SAMPLE TEST 7	0 MPa	0.2 mA/cm ²	1 hour	0-1000K
SAMPLE TEST 8	0 MPa	0.2 mA/cm ²	1 hour	0-1000K
SAMPLE TEST 9	0 MPa	0.2 mA/cm ²	1 hour	0-1000K

SAMPLE TEST 10	0 MPa	2 mA/cm ²	1 hour	0-1000K
SAMPLE TEST 11	0 MPa	2 mA/cm ²	1 hour	0-1000K
SAMPLE TEST 12	0 MPa	2 mA/cm ²	1 hour	0-1000K
SAMPLE TEST 13	50 MPa	0.02 mA/cm ²	1 hour	0-1000K
SAMPLE TEST 14	50 MPa	0.02 mA/cm ²	1 hour	0-1000K
SAMPLE TEST 15	100 MPa	0.02 mA/cm ²	1 hour	0-1000K
SAMPLE TEST 16	100 MPa	0.02 mA/cm ²	1 hour	0-1000K
SAMPLE TEST 17	150 MPa	0.02mA/cm ²	1 hour	0-1000K
SAMPLE TEST 18	150 MPa	0.02mA/cm ²	1 hour	0-1000K
SAMPLE TEST 19	300 MPa	0.02 mA/cm ²	1 hour	0-1000K
SAMPLE TEST 20	300 MPa	0.02 mA/cm ²	1 hour	0-1000K
SAMPLE TEST 21	600 MPa	0.02 mA/cm ²	1 hour	0-1000K
SAMLE TEST 22	600 MPa	0.02 mA/cm ²	1 hour	0-1000K

Table 2: List of all the dual-phase steels and the varying conditions

4 CHARACTERISATION OF DUAL PHASE MATERIAL

4.1 Chemical Composition Of The DP980MPa

Title: The details of the composition of the DP980 in weighted percentages.

MATERIAL	CHEMICAL COMPOSITION MIX IN WEIGHTED PERCENTAGES															
Chemical symbols of materials	C, %	Si, %	Mn, %	P, %	S, %	Cr, %	Al, %	Mo, %	Nb, %	V, %	Ti, %	B, %	Rp0.2, MPa	Rm, MPa	A5, %	A8, %
DP980	0.02	0.061	0.022	0.001	0.0007	0.038	0.079		0.04				650	1060		15.5

Table 3: List of all the chemical properties in weighted percentages of the dual-phase steel material used

4.2 Microstructure characterisation

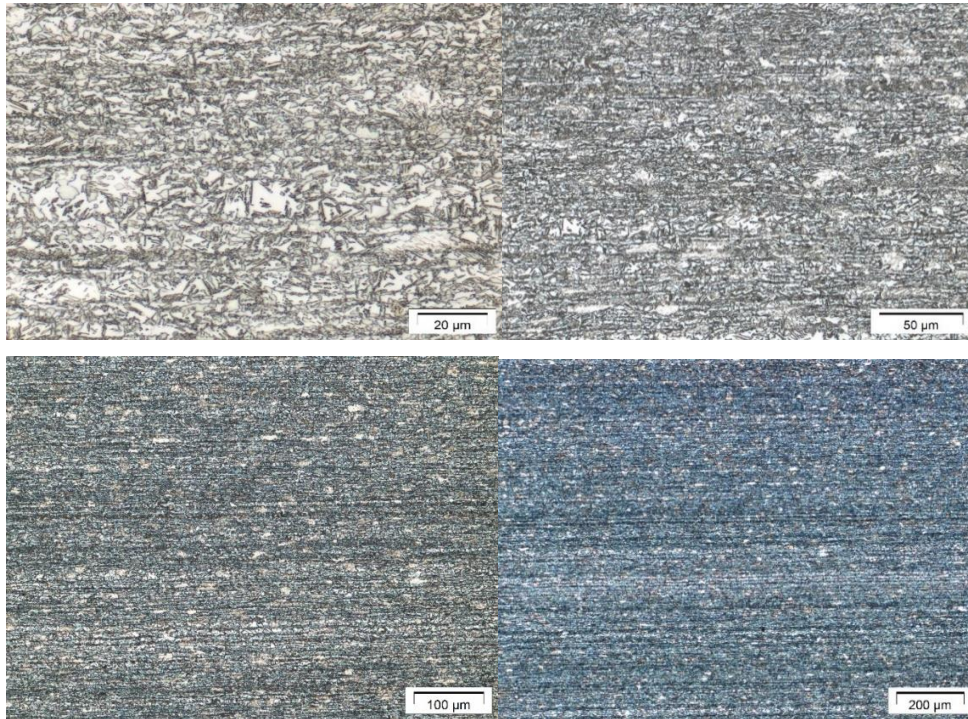


Figure 14: Microstructure of DP980 at four different magnifications

Figure 22 shows the images of the microstructures of the investigated DP steels. The images were taken from the central positions of the samples. The dark portions represent the martensite and the white portions are ferrite in the micrographs with four magnifications.

4.3 Characterisation of Dual-Phase Steel Material

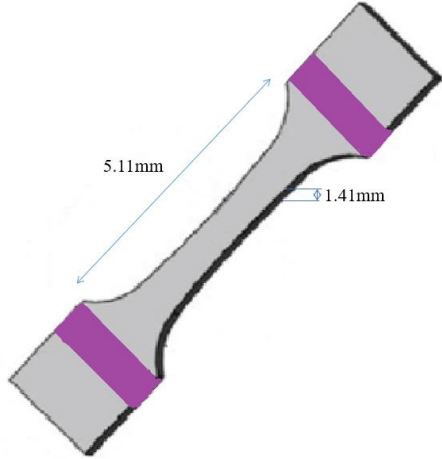


Figure 15: A typical shape DP steel for the experiment

5. DISCUSSION OF HYDROGEN'S INFLUENCE ON MECHANICAL PROPERTIES

5.1 Discussion of results from Thermal Desorption Spectroscopy

The results of Thermal Desorption Spectroscopy under several conditions. The following provides data on Dual phase steel that has been both charged by hydrogen and not charged. The hydrogen content is measured against temperature in the Thermal Desorption Spectroscopy. The curves obtained by SSRT lab tests provide information about the hydrogen desorption of the dual-phase steel. The figures provide the hydrogen desorption for dual-phase steel under varying currents and pressure.

5.1.1 Without Charging

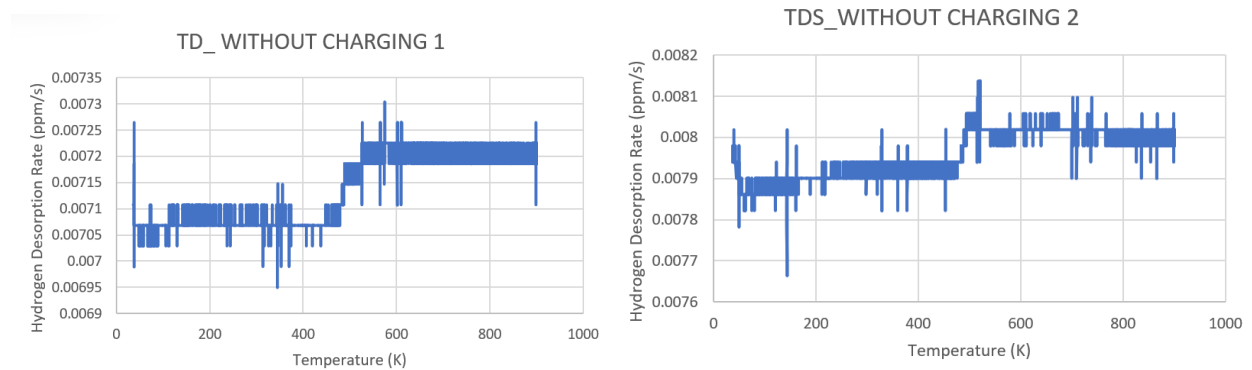


Figure 16: TDS graphs (1&2) of Hydrogen desorption rate in ppm/s against temperature in Kelvin of a DP980 weighted 11.956g without charging recorded in the laboratory.

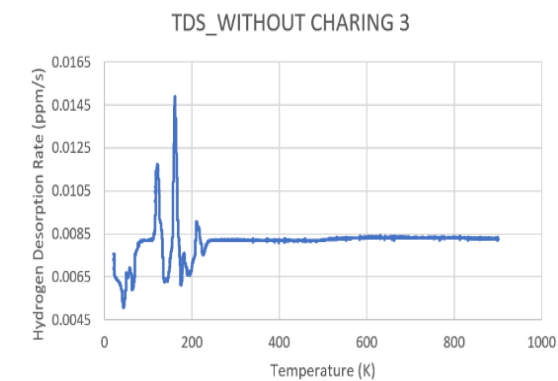


Figure 17: A TDS graph of Hydrogen desorption rate in ppm/s against temperature in Kelvin of a DP980 weighted 11.93g without charging recorded in the laboratory

5.1.2 Thermal Desorption Spectroscopy at $0.2\text{mA}/\text{cm}^2$ in 1 hour with 0MPa

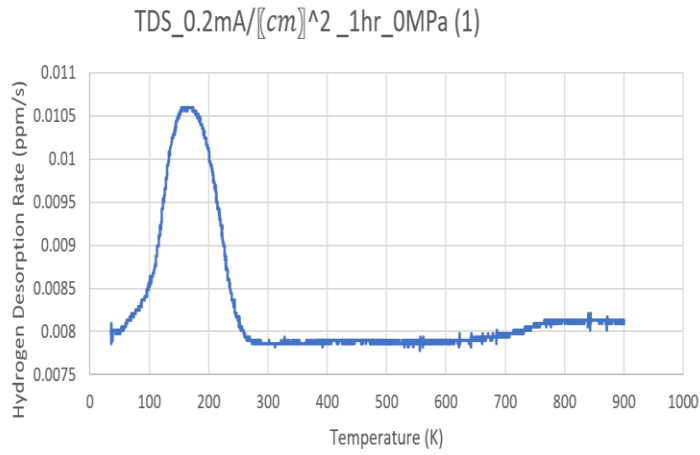


Figure 18: A TDS graph of Hydrogen desorption rate in ppm/s against temperature in Kelvin of a DP980 weighted 12.2154g.

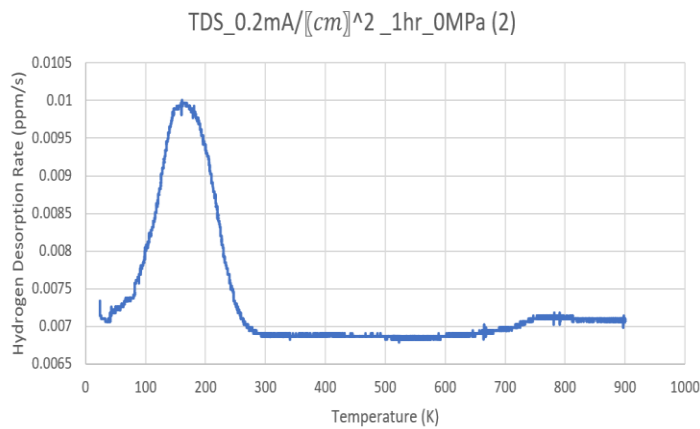


Figure 19: A TDS graph of Hydrogen desorption rate in ppm/s against temperature in Kelvin of a DP980 weighted 12.1728g recorded in the laboratory.

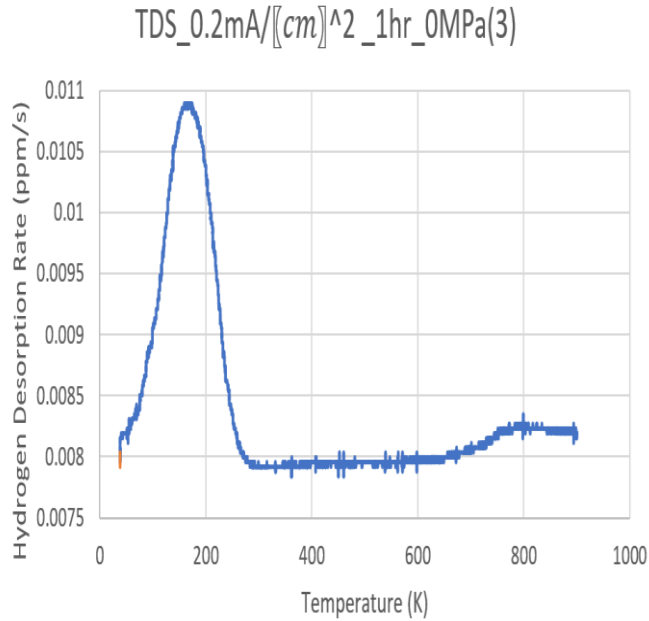


Figure 20: A TDS graph of Hydrogen desorption rate in ppm/s against temperature in Kelvin of a DP980 weighted 12.184g recorded in the laboratory.

5.1.3 Thermal Desorption Spectroscopy at $0.02\text{mA}/\text{cm}^2$ in 1 hour with 0MPa

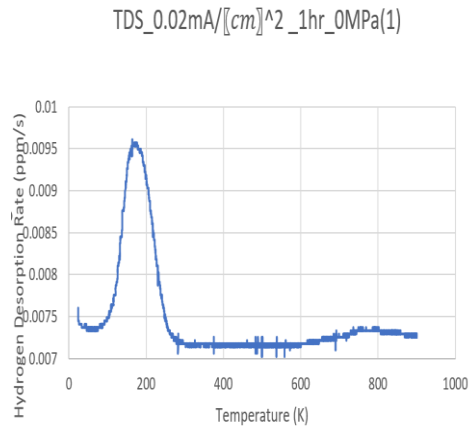


Figure 21: A TDS graph of Hydrogen desorption rate in ppm/s against temperature in Kelvin of a DP980 weighted 12.1523g recorded in the laboratory.

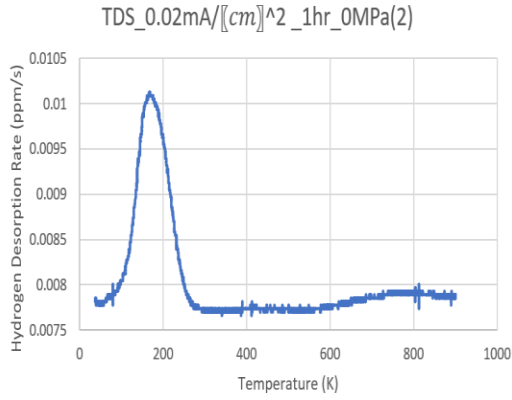


Figure 22:A TDS graph of Hydrogen desorption rate in ppm/s against temperature in Kelvin of a DP980 weighted 12.1833g recorded in the laboratory.

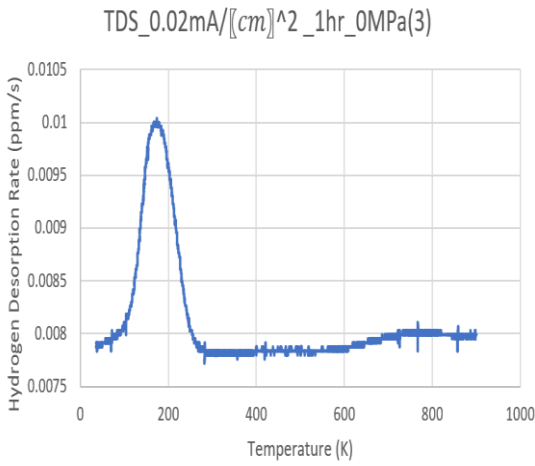


Figure 23:A TDS graph of Hydrogen desorption rate in ppm/s against temperature in Kelvin of a DP980 weighted 12.148g recorded in the laboratory.

5.1.4 Thermal Desorption Spectroscopy at $2\text{mA}/\text{cm}^2$ in 1 hour with 0MPa

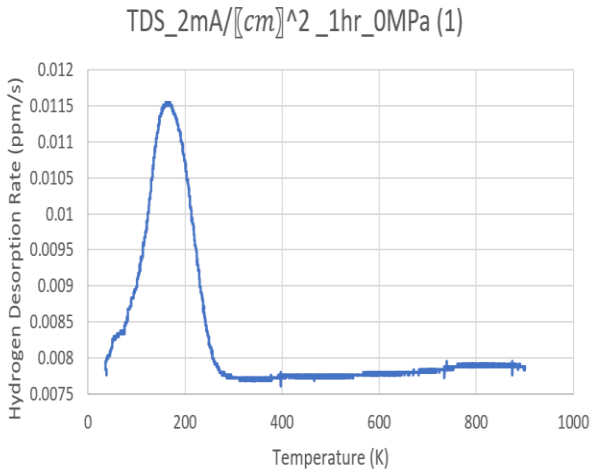


Figure 24: A TDS graph of Hydrogen desorption rate in ppm/s against temperature in Kelvin of a DP980 weighted 12.247g recorded in the laboratory.

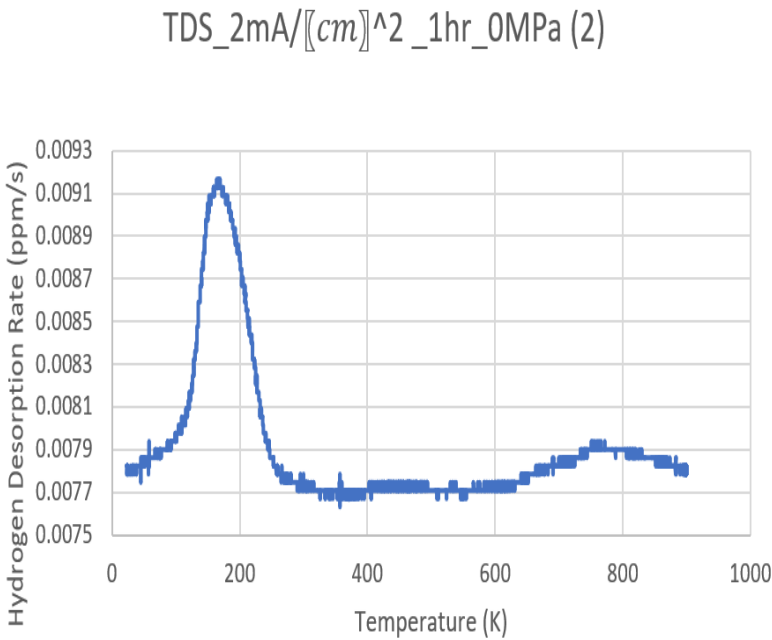


Figure 25: A TDS graph of Hydrogen desorption rate in ppm/s against temperature in Kelvin of a DP980 weighted 12.2086g recorded in the laboratory.

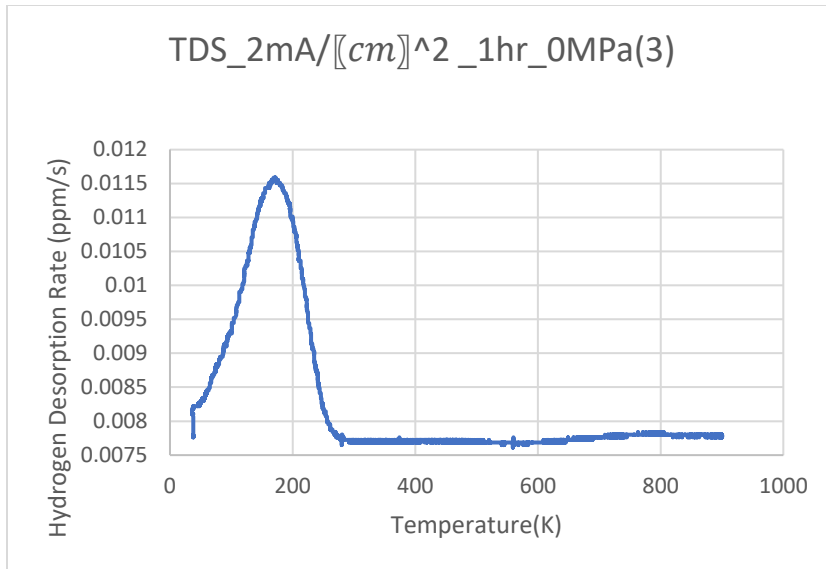


Figure 26: A TDS graph of Hydrogen desorption rate in ppm/s against temperature in Kelvin of a DP980 weighted 12.2458g recorded in the laboratory.

5.1.5 Thermal Desorption Spectroscopy at 0.2mA/cm² in 1 hour with 50MPa

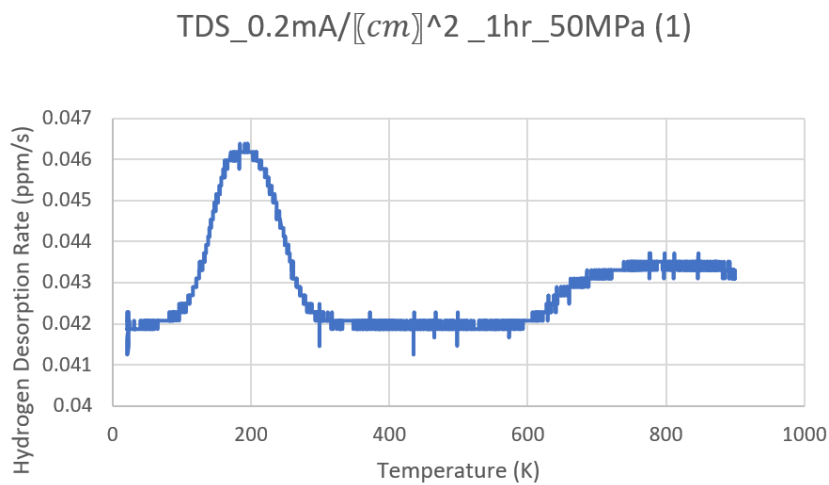


Figure 27: A TDS graph of Hydrogen desorption rate in ppm/s against temperature in Kelvin of a DP980 weighted 2.3134g recorded in the laboratory.

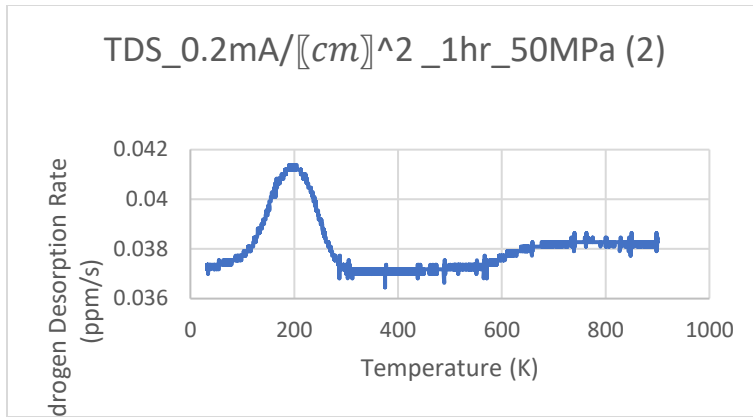


Figure 28: A TDS graph of Hydrogen desorption rate in ppm/s against temperature in Kelvin of a DP980 weighted 2.6053g recorded in the laboratory.

5.1.6 Thermal Desorption Spectroscopy at 0.2m/cm² in 1hour with 100MPa

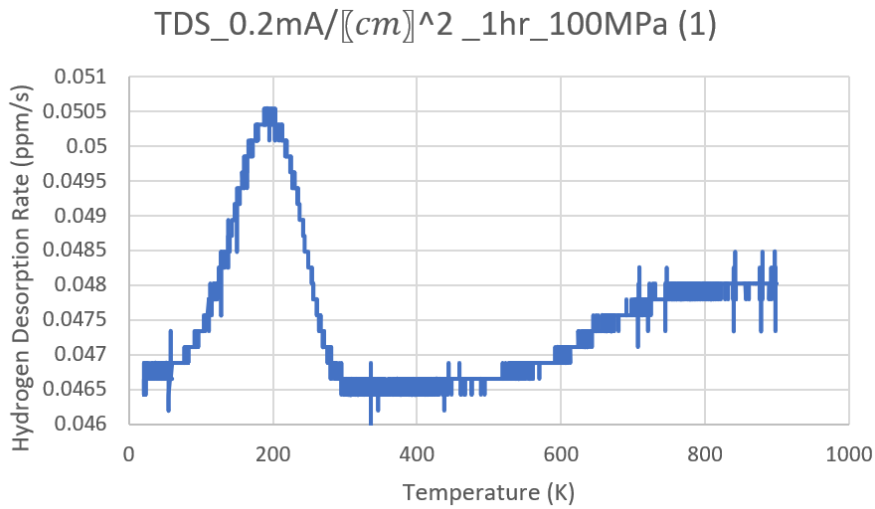


Figure 29: A TDS graph of Hydrogen desorption rate in ppm/s against temperature in Kelvin of a DP980 weighted 2.079g recorded in the laboratory.

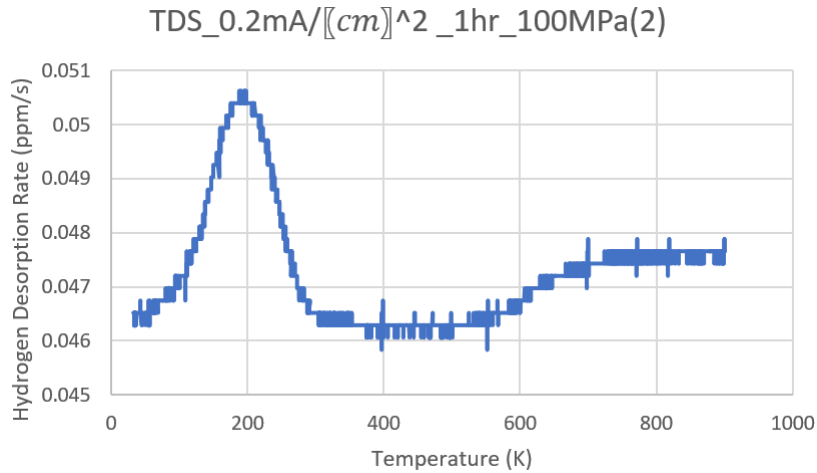


Figure 30: A TDS graph of Hydrogen desorption rate in ppm/s against temperature in Kelvin of a DP980 2.0851g recorded in the laboratory.

5.1.7 Thermal Desorption Spectroscopy at 0.2m/cm² in 1hour with 150MPa

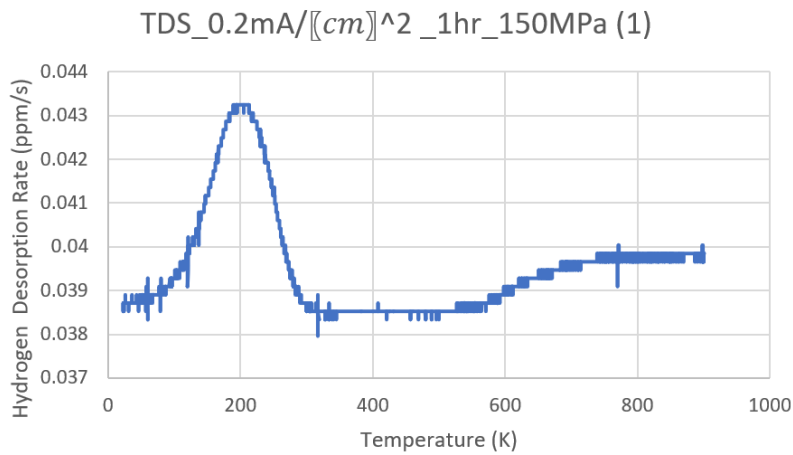


Figure 31: A TDS graph of Hydrogen content in ppm/s against temperature in Kelvin of a DP980 weighted 2.5282g recorded in the laboratory.

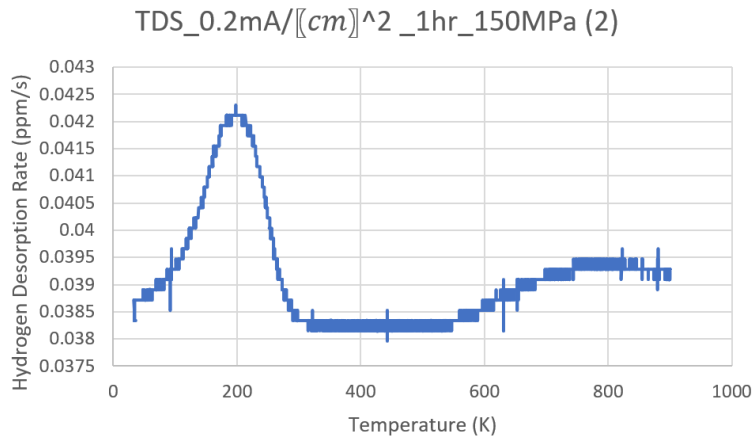


Figure 32: A TDS graph of Hydrogen desorption rate in ppm/s against temperature in Kelvin of a DP980 weighted 2.5281g recorded in the laboratory.

5.1.8 Thermal Desorption Spectroscopy at 0.2m/cm² in 1hour with 300MPa

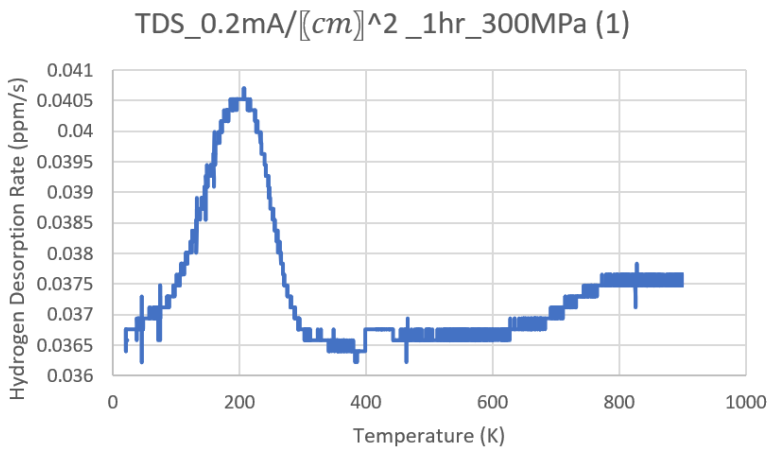


Figure 33: A TDS graph of Hydrogen desorption rate in ppm/s against temperature in Kelvin of a DP980 weighted 2.662g recorded in the laboratory.

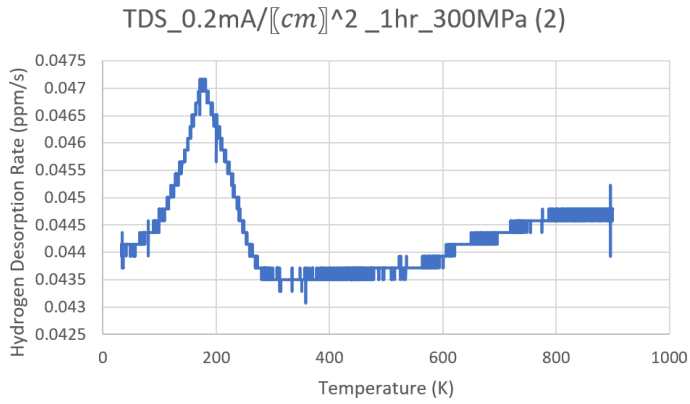


Figure 34: A TDS graph of Hydrogen desorption rate in ppm/s against temperature in Kelvin of a DP980 weighted 2.2165g recorded in the laboratory.

5.1.9 Thermal Desorption Spectroscopy at 0.2m/cm² in 1hour with 600MPa

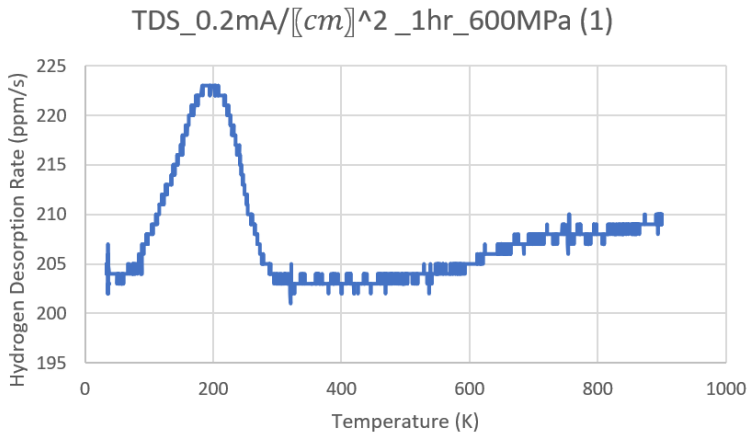


Figure 35: A TDS graph of Hydrogen desorption rate in ppm/s against temperature in Kelvin of a DP980 2.3384g recorded in the laboratory.

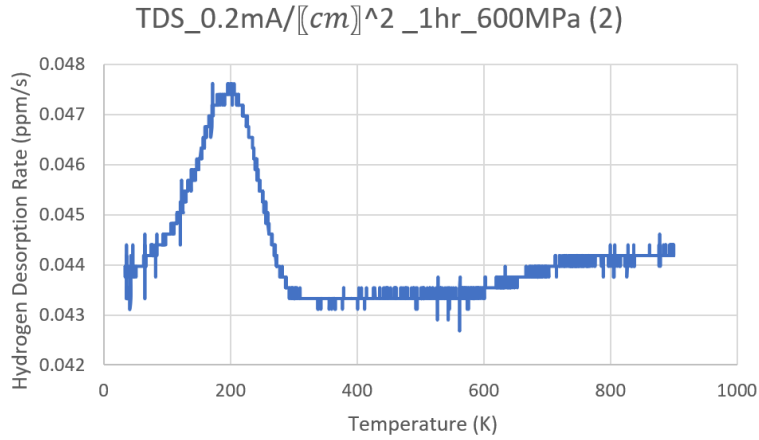


Figure 36: A TDS graph of Hydrogen desorption rate in ppm/s against temperature in Kelvin of a DP980 2.2254g recorded in the laboratory.

5.2.0 Combined results of all TDS graphs

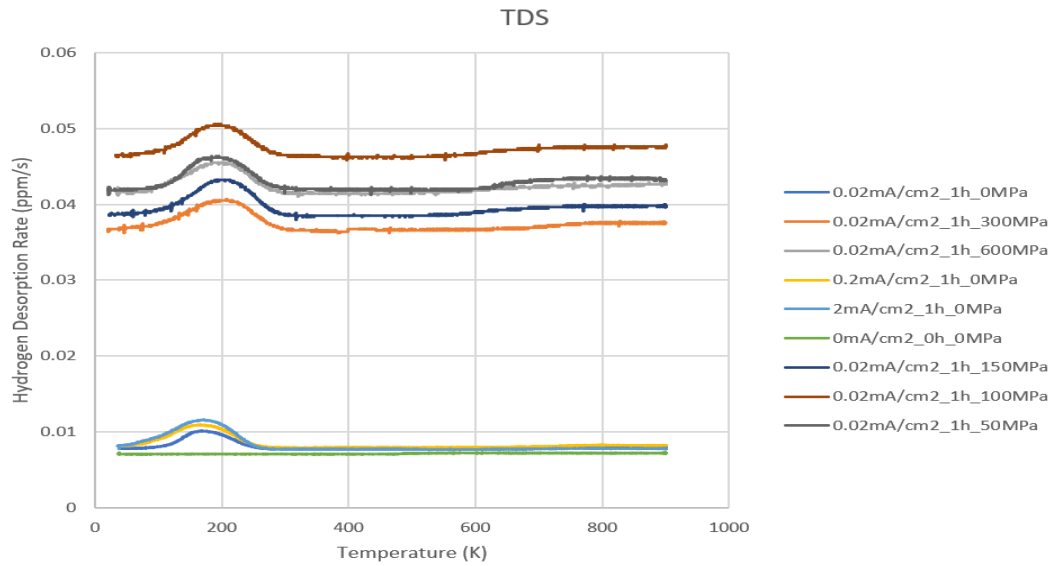


Figure 37: A TDS graph of all the combined varying conditions for hydrogen desorption rate in ppm/s against temperature in Kelvin.

5.2.1 Combined results of all TDS graphs with time as the x axis

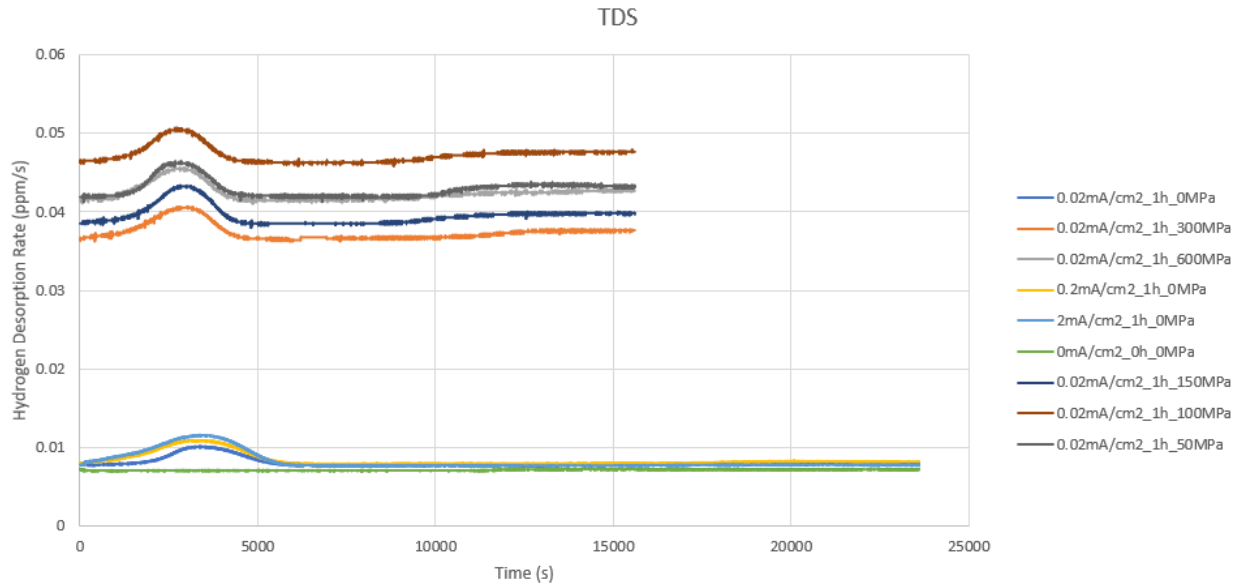


Figure 38: A TDS of all the combined varying conditions for hydrogen desorption rate in ppm/s against time in second.

5.3 Analysis of results from TDS

Figure 5.2.0 provides a combined graphical representation of TDS for nine kinds of dual-phase steels. The graph provides information about the varying hydrogen uptake and concentrations with and without hydrogen charging. The interpretation of the desorption curves from TDS provides meaningful information on diffusivity and deeply trapped hydrogen in Dual phase steel.

The varying conditions include temperature, pressure, time and charging density. The dual-phase steel's hydrogen-related behavior is about to be investigated against the behavior of the following parameters.

5.3.1 Temperature

From the figure 5.2.0, as shown by material without charging, 0 m/cm^2 in 1hour with 0 MPa, the desorbed hydrogen at temperatures is constant below at all temperature has a relatively low quantity of 0.007068135 ppm/s. The desorbed hydrogen at this low temperature is considered as diffusive hydrogen, it is the reversible trapping site. At that temperature the desorption rates are higher due to the lowering of the activation energies of the irreversible sites. The irreversible site of dual-phase steels from the graph has lower binding energies, so it is easy for hydrogen to desorb at lower temperatures. For the instance with several charging conditions, the graph depicts that significant desorption first occurred between 77K and 310K and another upsurge after 600K. Clearly, temperature influences the desorption rate.

5.3.2 Pressure

From figure 5.2.0, pressure has varying effects on the desorption rate. Clearly, for the test with no pressure the graph had desorption rates less than 0.02ppm/s. For the other instance where there was varying pressure, the pressure varied with the other conditions. All the test with pressures ranging from 50MPa to 600MPa experienced a desorption rate higher than 0.03ppm/s since the higher pressures increases the concentration of hydrogen in the environment surrounding the DP steel specimen. This results in a higher concentration gradient between the trapping sites within the material and the surrounding enhancing the desorption rate. Higher pressure in the environment can lead to enhanced availability of hydrogen in the desorption rate from trapping sites in the dual-phase material.

5.3.3 Charging densities

Figure 5.2.0 shows different curves corresponding to the varying temperatures. This informs of the effects of the varying current densities and their effects on the desorption rates. For higher charging densities there is a greater concentration of hydrogen within the material's trapping sites. The charging densities have a direct impact on the hydrogen as higher charging densities can lead to increased mobility and diffusion. For samples with other similar conditions, the material with higher charging densities exhibited higher desorption rates.

5.3.4 Combined effects

The samples were all pre-charged for 1 hour and measured up to 1000K in the various TDS tests. The quantity of diffusivity varies with varying charge densities, pressures, and temperatures. From the graph at higher temperature, hydrogen is released from trapping sites. Coupled with higher charging densities, the desorption rate occurs faster because the desorption rates increase due to faster desorption kinetics.

5.4 Evaluation of the susceptibility to HE and the consequences of using Dual Phase Steel for hydrogen application in the energy sector

Many industries, including the production of automotive components, the transportation sector, and the petrochemical sector, use dual-phase steel materials. When working materials come into contact with hydrogen during operation, embrittlement of the material occurs if hydrogen is present in the operating environment. To lessen this, various preventive measures must be taken so that materials cannot be harmed by hydrogen and that the effect further does not damage the mechanical properties of materials. From the factors causing hydrogen-included cracking (HIC), it can be summarised that since hydrogen desorption conditions are mostly conditions triggered in the HIC, the material must be made to fully withstand

Particularly when hydrogen content was low, observations made by partial phase transition and tempering were more resistant to HE than TM without significantly losing strength. The susceptibility of DP steels to HE during the application in the energy sector is inevitable, thus the material needs to be fully adapted with several processes to be able to be used in the energy sector.

6. CONCLUSION AND RECOMMENDATION

The TDS was used to analyse the absorptibility of hydrogen and its potential effects on the mechanical properties of a dual-phase steel. It was observed that the DP980 experienced hydrogen absorption and consequently the mechanical qualities (strength and ductility) will be affected. From the microstructure analysis of the cracked material in the literature, the HE impacts on the material were quite evident.

The effect of interstitial hydrogen on the elastic behavior of metals has been studied, and the findings accurately quantify the variation in elastic behavior of various metals including DP steels, so when the DP steels are exposed to a hydrogen-rich environment the mechanical properties will be compromised. Thus the environment for the transportation of hydrogen should be well either properly coated or alloyed to prevent failure.

It was observed that when dual-phase steels are charged under pressures and varying temperatures, the hydrogen desorption in the material is mainly in the reversible sites which have low binding energies. Only a small quantity of hydrogen is desorbed in the irreversible trapping sites. In other terms, the diffusivity of hydrogen in dual-phase steels is mostly due to the hydrogen-induced cracking behaviors in the material. The presence of hydrogen in a the dual phase steel can enhance the mobility of the dislocation. TDS results suggest the material has reversible hydrogen trapping sites indicating they are highly susceptible to hydrogen-related failure, and it is not ideal for hydrogen transportation applications.

By conducting additional desorption tests under no charging conditions, the bulk diffusion graphs were verified. As a result, the bulk diffusion graphs are ideal for explaining hydrogen diffusion, trapping, and desorption in DP steels.

It is discovered that the only three variables that permit comparison of TDS experiments from the literature are temperature, current density, and pressure.

Additionally, literature research was done on the potential role of metal coatings and alloying as hydrogen diffusion barriers for DP steels, and comparisons were made with experimental data from the literature for several materials. Hydrogen desorption is somewhat prevented by the effective diffusion coefficient of about $10^{-9} \text{ mm}^2/\text{s}$. Regardless, experimental studies are required to enhance the bulk diffusion model and fully comprehend the function of coatings. The literature also recommends that reduction of the absorption rate by alloying the steel materials, for full integration of the dual phase steel in the energy sector the alloying emphasised in the literature could be adopted.

The effect of hydrogen's presence in the lattice affecting the elastic interaction of dual-phase steel has been investigated in several studies. Here are some key findings worth applicable in this research. Due to the

elastic stress, the crystallographic lattice of dual-phase steel expands, which increases hydrogen diffusivity in the material. The applied elastic tensile stress enhances the rate of desorption of diffusible hydrogen, increasing hydrogen diffusion kinetics in dual-phase steel. Hydrogen embrittlement affects high-strength ferrite/martensite dual-phase (DP) steels and the associated micromechanisms that lead to failure have not been fully understood yet. Hydrogen can be attracted elastically to a loaded crack tip, leading to supersaturation and precipitation of a hydride, which can cause hydrogen embrittlement in steels hence the coating and alloying of dual-phase steel surfaces are crucial for the reduction of HE in materials. The HE resistance can be made with surface nitriding, and carburizing: this is to reduce lattice spacing by stabilising austenite, by surface coating with Ni, Al, Cu coatings, hard films Si_3N_4 , Al_2O_3 , and TiN.

REFERENCE

- [1] www.iea.blob.core.window.net, GlobalEnergyReviewCO2Emissionsin2021 – Gloval emissions rebound sharply to highest ever level.
- [2] www.un.org/en/chronicle/article/goal-7-ensure-access-affordable-reliable-sustainable-and-modern-energy-all, April 2015, No. 4 Vol. LI, Beyond 2015.
- [3] <https://www.iea.org/energy-system/low-emission-fuels/hydrogen>, Energy system – low emission fuels-hydrogen
- [4] US Department of Energy (2020). Road Map to a US Hydrogen Economy: Reducing emission and driving growth across the nation
- [5] Sankara P. (2014). Mechanisms. In Corrosion Control in Oil and Gas Industry. Gulf Professional Publishing, USA : 249-300
- [6] www.iea.org/data-and-statistics/charts/global-annual-average-change-in-fossil-fuels-production-by-fuel-2018-2019-and-2019-2020,) Global annual average change in fossil fuels production by fuel
- [7] Hren R., Vujanović A., Fan V. Y., Klemeš J. J., Krajnc D. & Čuček L. (2023). Hydrogen production, storage and transport for renewable energy and chemicals: An environmental footprint assessment. *Renewable and Sustainable Energy Reviews*, **Volume 173**: 113113p
- [8] Meroño E., (2020). European Association for Storage of Energy
- [9] IEA (2021). Net Zero by 2050: A Roadmap for the Global Energy Sector, International Energy Agency, Paris Cedex 15, France.
- [10] IEA (2023). Renewables 2022: Analysis and forecast to 2027, International Energy Agency, Paris Cedex 15, France
- [11] <https://www.twi-global.com/technical-knowledge/faqs/what-are-the-pros-and-cons-of-hydrogen-fuel-cells>, What are the pros and cons of hydrogen fule cells?
- [12] Knosala K., Kotzur L., Röben T.C.F., Stenzel P., Blum L., Robinius M. & Stolten D. (2021). Hybrid Hydrogen Home Storage for Decentralized Energy Autonomy. *International Journal of Hydrogen Energy*, Volume 46, Issue 42, 21748-21763p.
- [13] Sánchez A. L. & Williams A. F. (2014). Recent Advances in understanding of flammability characteristics of hydrogen, *Progress in Energy and Combustion Science*. Volume 41, 1-55p.
- [14] Jolly W. L. (2023). Hydrogen: Chemical Element. *The Editors of Encyclopaedia Britannica*

- [15]&[16] R. Gerboni (2016). Introduction to hydrogen transportation: Safety issues. *Compendium of Hydrogen Energy*.
- [17] Fonstein N. (2017). Dual Phase Steels: Introduction. *Automotive Steels, Woodhead Publishing, 169-216p.*
- [18] Ayadi S., Hadji A. & Hakan K., Selman D. (2020). Microstructure and wear behavior of a Cr-Mo-Nb alloyed manganese steel, *Journal of Materials Research and Technology, Volume 9, Issue , 11545-11562p*
- [19] Eyres D.J. & Bruce G.J. (2012). Tanker Construction. *Ship Construction (Seventh Edition), 265-277p.*
- [20] Benzing J.T., Poling W.A., Pierce D.T., Bentley J., Findley K.O., Raabe D. & Wittig J.E. (2017). Effects of Strain Rate On Mechanical Properties and Deformation Behaviour Of an Austenitic Fe-25Mn-3Al-3Si TWIP-TRIP Steel.
- [21] Horvath C.D. (2021). Chapter 2 - Advanced Steels For Lightweight Automotive Structures: Complex-phase steels. *Materials, Design and Manufacturing for Lightweight Vehicles, Woodhead Publishing, 39-95p.*
- [22] Easton M.A. & StJohn D.H. (2011). Grain Refinement in Alloys: Novel Approaches. *Encyclopedia of Materials, Science and Tehcnology.*
- [23] Hilditch T.B., de Souza T., & Hodgson P.D. (2015). Properties and automotive applicaations of Advanced High-Strength Steels (AHSS), *Woodhead Publishing, 9-28p.*
- [24] Shakerifard B., Lopez G.J., Legaza M. C.T., Verleysen P., Kestens L.A.I. (2019). Strain Rate Dependent Dynamic Mechanical Response Of Bainitic Multiohase Steels, *Materials Science and Engineering: A, Volume 745, 279-290p.*
- [25] Shome M., Tumuluru M. (2015). Introduction to welding and joining of advanced high-strength steels (AHSS), *Woodhead Publsiing, 1-8p.*
- [26] Nayak S.S., Biro E. & Zhou Y. (2015). Laser welding of advanced high-strength steels (AHSS), *Woodhead Publishing, 71-92p.*
- [27] Zhang W. & Xu J. (2022). Advanced Lightweight materials for Automobiles: A review, *Material & Design, Volume 221, 110994p.*

- [28] Tehrani-Moghadam H.G., Jafarian H.R., Heidarzadeh A., Eivani A.R., Do H. & Park N. (2020). Achieving extraordinary strength and ductility in TRIP steels through stabilising of austenite up to 99.8% by friction stir welding, *Material Science and Engineering: A, Volume 773*, 138876p.
- [29] Xiong Z.P., Kostryzhev A.G., Saleh A.A., Chen L. & Pereloma E.V. (2016). Microstructures and Mechanical properties of TRIP steel produced by strip casting simulated in the Laboratory, *Materials Science and Engineering: A, Volume 664*, 26-24p.
- [30] Järvinen H., Honkanen M., Järvenpää M. & Peura Pasi. (2018). Effects of paint baking treatment on the properties of press hardened Boron steels, *Journal of Materials Processing Technology, Volume 252*, 90-104p.
- [31] Christodoulou P. (2017). Effects of Retained Austenite Transformation on The Fatigue Behaviour of Aluminum containing TRIP Steel, *ResearchGate. Thesis*.
- [32] Somers M.A.J. & Christiansen T.L. (2015). Gaseous processes for low temperature surface hardening of stainless steel, *Thermochemical Surface Engineering of Steel: Woodhead Publishing*, 581-614p.
- [33] Horvath C.D. (2021). Chapter 2 - Advanced Steels For Lightweight Automotive Structures: Cold-rolled martensitic and heat-treated boron steels. *Materials, Design and Manufacturing for Lightweight Vehicles (Second Edition)*, Woodhead Publishing. 39-95p.
- [34] Wanhill R.J.H., Byrnes R.T & Smith C.L. (2011). 16 – Stress corrosion cracking (SCC) in aerospace vehicles, *Woodhead Publishing Series in Metals and Surface Engineering, Stress Corrosion Cracking*, 608-650p.
- [35] <https://www.hobartbrothers.com/resources/technical-guides/stainless-steel-technical-guide/class-i-martensitic-stainless-steels/>, Class I – Martensitic Stainless Steels, *Stainless Steel Technical Guide*.
- [36] Murakami Y. (2019). 17 – Martensitic Stainless Steels, *Metal Fatigue (Second Edition)*, Academic Press, 431-451p.
- [37] Dawes C. (1992). Chapter 4 – Materials: In Woodhead Publishing Series in Welding and Other Joining Technologies,, *Laser Welding*, Woodhead Publishing. 51-77p.
- [38] Esaklul K.A (2017). 13- Hydrogen Damage, *In Woodhead Publishing Series in Energy, Trends in Oil and Gas Corrosion Research and Technologies*, Woodhead Publishing, 315-340p.

- [39] Li L.X., Wang Y.H., Wang W.J., Lui J.Y., Xu Z.Q. & Du F.S. (2021). Mechanism and Prediction of hydrogen embrittlement based on complex phase structure of chromium alloy steel, *Materials Science and Engineering: A*, Volume 822, 141546p.
- [40] Yaktiti A., Dreano A., Carton J.F. & Christien F. (2022). Hydrogen diffusion and trapping in a steel containing porosities.
- [41] Mohtadi-Bonab M.A. & Masoumi M. (2023). Different aspects of hydrogen diffusion behavior in pipeline steel, *Journal of Materials Research and Technology*, Volume 23, 4762-4783p.
- [42] Peral L.B., Díaz A., Alegre J.M. & Cuesta I.I. (2023). Hydrogen uptake and diffusion kinetics in a quenched and tempered low carbon steel: Experimental and numerical study, *International Journal of Hydrogen Energy*.
- [43] Hedenstedt K., Simic N., Wildlock M. & Ahlberg E. (2016). Kinetic study of the hydrogen evolution reaction in slightly alkaline electrolyte on mild steel, goethite and lepidocrocite, *Journal of Electroanalytical Chemistry*, Volume 783, 1-7p.
- [44] Nikulshina V., Hirsch D., Mazzotti M. & Steinfeld A. (2006). CO₂ capture from air and co-production of H₂ via the Ca(OH)₂-CaCO₃ cycle using concentrated solar power-Thermodynamic analysis, *Energy*, Volume 31, 1715-1725p.
- [45] Zhou B., Ou P., Rashid T. R., Vanka S., Sun K., Yao L., Sun H., Song J. & Mi Z. (2020). Few-Atomic-Layers Iron for Hydrogen Evolution from Water by Photoelectrocatalysis, *Volume 23, Issue 10*, 101613p.
- [46] Murakami Y. (2019). 21- Hydrogen embrittlement, *Metal Fatigue (Second Edition)*, Academic Press, 567-607p.
- [47] Jin X., Hu G., Wang L. & Wang H. (2020). Characterisation of surface layers of oxidation-reduction treated Si and Mn added advanced high strength steel, *Surface and Coatings Technology*, Volume 382, 125172p.
- [48] Delpupo M.N., Inés M.N., Candia G., Asmus C. & Mansilla G. A. (2015). Relationship between the electrogalvanized stages and income of hydrogen in low carbon wire steel. *International Congress of Science and Technology of Metallurgy and Materials, SAM-CONAMET 2014. Procedia Material Science* 9, 171-176p.
- [49] Hafsi Z., Mishra M. & Elaoud S. (2018). Hydrogen embrittlement of steel pipelines during transients, *Procedia Structural Integrity*, Volume 13, 210-217p.

- [50] Lei Y., Hosseini E., Lui L., Scholes C.A. & Kentish S.E. (2022). Internal polymeric coating materials for preventing pipeline hydrogen embrittlement and a theoretical model of hydrogen diffusion through coated steel. *International Journal of Hydrogen Energy*, Volume 47, Issue 73, 31409-31419.
- [51] Ahmad Z. (2006). Chapter 10 – Atmospheric Corrosion: Principles of Corrosion Engineering and Corrosion Control, *Butterworth-Heinemann*, 550-575.
- [52] Hafsi Z., Mishra M. & Elaoud. (2018). Hydrogen embrittlement of steel pipelines during transients, *Procedia Structural Integrity*, Volume 13, 210-217.
- [53] Lei Y., Hosseini E., Lui L., Scholes C. A. & Kentish S.E. (2022). Internal polymeric coating materials for preventing pipeline hydrogen diffusion through coated steel, *International Journal of Hydrogen Energy*, Volume 47, Issue 73, 31409-31419p.
- [54] Louthan M. R. & Caskey G. R. (1976). Hydrogen transport and embrittlement in structural metals, *International Journal of Hydrogen Energy*, Volume 1, Issue 3, 291-305p.
- [55] King R. A. (2017). 11 – Sulfide stress cracking, *In Woodhead Publishing Series in Energy, Trends in Oil and Gas Corrosion Research and Technologies*, Woodhead Publishing, 271-294p.
- [56] Marchi S. C. Somerday B.P. & Robinson S.L. (2007). Permeability, solubility and diffusivity of hydrogen isotopes in stainless steels at high gas pressures, *International Journal of Hydrogen Energy*, Volume 32, Issue 1, 100-116p.
- [57] Chalfoun D. R., Kappes M. A., Bruzzoni P., & Iannuzzi M. (2022). Hydrogen solubility, diffusivity, and trapping in quenched and tempered Ni-containing steels, *International Journal of Hydrogen Energy*, Volume 47, Issue 5, 3141-3156p.
- [58] Drexler A., Konert F., Sobol O., Rhode M., Domitner J., Sommitsch C. & Böllinghaus T. (2022). Enhanced gaseous hydrogen solubility in ferritic and martensitic steels at low temperatures, *International Journal of Hydrogen Energy*, Volume 47, Issue 93, 39639-39653p.
- [59] X. Guo, Influences of microstructure, alloying elements and forming parameters on delayed fracture in TRIP/TWIP-aided austenitic steels. *PhD. thesis, RWTH-Aachen University, 2012.*
- [60] Sanchez J., Ridruejo A. & de Andres P. L. (2020). Diffusion and trapping of hydrogen in carbon steel at different temperatures, *Theoretical and Applied Fracture Mechanics*, Volume 110, 102803p.

- [61] Zarnas P. D., Dingreville R. & Qu J. (2018). Mechanics of point defects diffusion near dislocations and grain boundaries: A chemomechanical framework, *Computational Materials Science, Volume 144*, 99-112p.
- [62] Pisarev A.A. (2012). 1 – Hydrogen adsorption on the surface of metals, *In Woodhead Publishing Series in Metals and Surface Engineering, Gaseous Hydrogen Embrittlement of Materials in Energy Technologies, Woodhead Publishing, Volume 1*, 3-26p.
- [63] Eliezer D. & Silverstein R. (2018). Recent Studies of Hydrogen Embrittlement in Structural Materials, *Procedia Structural Integrity, Volume 13*, 2233-2238p.
- [64] Luo F., Liu Q., Huang J., Xiao H., Gao Z., Ge W., Wang Y. & Wang C. (2023). Effects of lattice strain on hydrogen diffusion, trapping and escape in bcc iron from ab-initio calculations, *International Journal of Hydrogen Energy, Volume 48, Issue 22*, 8198-8215p.
- [65] Yang J., Zhang D., Zhang H., Shang Z., Wang H., Meng C., Lui W. & Yue M. (2023). Effects of hydrogen pressure on hydrogenation and pulverization behavior of Sm (CoFeCuZr)_z ingot and strip casting flake, *Journal of alloys and compounds, Volume 930*, 167427p.
- [66] Chen Y., Xu Z., Zhang X., Zhang T., Tang J., Sun Z., Sui Y. & Han X. (2021). Irreversible hydrogen embrittlement study of B1500HS high strength boron steel, *Material & Design, Volume 199*, 109404p.
- [67] Esaklul K. A. (2017). 13 – Hydrogen damage, *In Woodhead Publishing Series in Energy, Trends in Oil and Gas Corrosion Research and Technologies, Woodhead Publishing*, 315-340p.
- [68] Lynch S.P. (2011). 2 – Hydrogen embrittlement (HE) phenomena and mechanisms, *In Woodhead Publishing Series in Metals and Surface Engineering, Stress Corrosion Cracking, Woodhead Publishing*, 90-130p.
- [69] King A. R. (2017). 11 – Sulfide stress cracking, *In Woodhead Publishing Series in Energy, Trends in Oil and Gas Corrosion Research and Technologies, Woodhead Publishin* , 271-294p.
- [70] Xing X., Cheng R., Cui G., Lui J., Gou J., Yang C., Li Z. & Yang F. (2021). Quantification of the temperature threshold of hydrogen embrittlement in X90 pipeline steel, *Materials Science and Engineering: A, Volume 800*, 140118p.
- [71] Lynch S.P. (2011). 2 – Hydrogen embrittlement (HE) phenomena and mechanisms, *In woodhead Publishing*

- [72] Wang C., Zhang J., Liu C., Hu Q., Zhang R., Xu X., Yang H., Ning Y. & Li Y. (2023). Study on hydrogen embrittlement susceptibility of X80 steel through in-situ gaseous hydrogen permeation and slow strain rate tensile tests, *International Journal of Hydrogen Energy*, Volume 48, Issue 1, 243-256p.
- [73] Okuno K. & Takai K. (2023). Determination of hydrogen diffusibility and embrittlement susceptibility of high-strength steel evaluated at different temperatures based on the local equilibrium theory, *Acta Materialia*, Volume 246, 118725p.
- [74] Zvirko O. (2022). Anisotropy of hydrogen embrittlement in ferrite-pearlitic steel considering operational degradation, *Procedia Structural Integrity*, Volume 42, 522-528p.
- [75] Ouellette R. J. & Rawn J. D. (2018). 15 – Methods for Structure Determination Nuclear Magnetic Resonance and Mass Spectrometry, *Organic Chemistry (Second Edition)*, Academic Press, 427-461p.
- [76] Birnbaum H.K. & Sofronis P. (1994). Hydrogen-enhanced localized plasticity- a mechanism for hydrogen related fracture, *Material Science and Engineering: A*, Volume 176, Issue 1-2, 191-202p.
- [77] Huang S., Zhang Y., Yang C. & Hu Hui. (2020). Fracture strain model for hydrogen embrittlement based on hydrogen enhanced localized plasticity mechanism, *International Journal of Hydrogen Energy*, Volume 45, Issue 46, 25541-25554p.
- [78] Cem Ö., Mubashir M., Alfred L., Fan Z., Gary S. H., Robin K., Francesco C., Hadeel H., Bora D., Ulf K., Dirk L. E., Edvin L. & Jinshan P. (2023). The causation of hydrogen embrittlement of duplex stainless steel: Phase instability of the austenite phase and ductile-to-brittle transition of the ferrite phase – Synergy between experiments and modelling, *Corrosion Science*, Volume 217, 2023, 111140, ISSN 0010-938X, <https://doi.org/10.1016/j.corsci.2023.111140>.
- [79] Sunil B. & Rajanna S. (2020). Evaluation of mechanical properties of ferrite-martensite DP steels produced through intermediate quenching technique, *SN Applied Sciences*, Volume 2, Issue 8, 1461p.
- [80] Meada R., Wang Z., Ogawa T. & Adachi Y. (2020). Stress-strain partitioning behavior and mechanical properties of dual-phase steel using finite element analysis, *Materials Today Communications*, Volume 25, 101658p, ISSN 2352-4928.
- [81] Reddy K. S., Govindaraj Y. & Neelakantan L. (2023). Hydrogen diffusion kinetics in dual-phase (DP 980) steel: The role of pre-strain and tensile stress, *Electrochimica Acta*, Volume 439, 141727p, ISSN 0013-4686.

- [82] Massone A. & Kiener D. (2022). Prospects of enhancing the understanding of material-hydrogen interaction by novel in-situ and in-operando methods, *International Journal of Hydrogen Energy*, Volume 47, Issue 17, 10097-10111p, ISSN 0360-3199.
- [83] Inkson B. J. (2016). 2 – Scanning electron microscopy (SEM) and transmission electron microscopy (TEM) for materials characterization, *Material Characterisation Using Nondestructive Evaluation (NDE) Methods*, Woodhead Publishing, 17-43p, ISBN 9780081000403.
- [84] Mehrban N. & Bowen J. (2017). 5 – Monitoring biomineralization of biomaterials in vivo, *Monitoring and Evaluation of Biomaterials and their Performance in Vivo*, Woodhead Publishing, 81-110p, ISBN 9780081006030.
- [85] Lewin-Kretzchmar U., Efer J. & Engewald W. (2000). Explosive | Liquid Chromatography, *Encyclopedia of Separation Science*, Academic Press, 2767-2782, ISBN 9780122267703.
- [86] Aboura Y., Garner A. J., Euesden R., Barrett Z., Engel C., Holroyd N. J. H., Prangnell P. B. & Burnett T. L. (2022). Understanding the environmentally assisted cracking (EAC) initiation and propagation of new generation 7xxx alloys using slow strain rate testing, *Corrosion Science*, Volume 199, 110161p, ISSN 0010-938X.
- [87] Zhang F., Ruimi A., Wo C. P. & Field D. P. (2016). Morphology and destruction of Martensite in dual phase (DP980) steels and its relation to the multiscale mechanical behavior, *Materials Science and Engineering: A*, Volume 659, 93-103p, ISSN 0921-5093.
- [88] Vermeij T., Mornout C. J. A., Rezazadeh V. & Hoefnagels J. P. M. (2023). Martensite plasticity and damage competition in dual-phase steel: A micromechanical experimental-numerical study, *Acta Materialia*, Volume 254, 119020, ISSN 1359-6454.
- [89] Montoya-Rangel M., Garza-Montes-de-Oca N. F., Gaona-Tiburcio C. & Almeraya-Calderón, Corrosion mechanism of advanced high strength dual phase steels by electrochemical noise analysis in chloride solutions, *Materials Today Communications*, Volume 35, 105663p, ISSN 2352-4928.
- [90] Reddy S. K., Govindaraj Y. & Neelakantan L. (2023) Hydrogen diffusion kinetics in dual phase (DP 980) steel: The role of pre-strain and tensile stress, *Electrochimica Acta*, Volume 439, 141727p, ISSN 0013-4686.
- [91] Li X., Wang Y., Li B. Zhang P. & Song X. (2015). Effects of cathodic hydrogen-charging current density on mechanical properties of prestrained high strength steels, *Materials Science and Engineering: A*, Volume 641, 45-53p, ISSN 0921-5093.

- [92] Mertens G., Duprez L., De Cooman B. & Verhaege M. (2007). Hydrogen Absorption and Desorption in Steel by Electrolytic Charging, *Advanced Materials Research, Volume 15*, 816-821p.
- [93] Ogawa Y., Hosoi H., Tsuzaki K., Redarce T., Osamu T. & Matsunaga H. (2020). Hydrogen, as an alloying element, enables a greater strength-ductility balance in an Fe-Cr-Ni-based, stable austenite stainless steel, *Acta Materialia, Volume 1997*, 181-192p, ISSN 1359-6454, doi: <https://doi.org/10.1016/j.actamat.2020.08.024>.
- [94] Xu J., Yu C., Lu H., Wang Y., Luo C., Xu G. & Suo J. (2019). Effects of alloying elements and heat treatment on hydrogen diffusion in SCRAM steels, *Journal of Nuclear Materials, Volume 516*, 135-143p, ISSN 0022-3115, <https://doi.org/10.1016/j.jnucmat.2019.01.019>.
- [95] Alp T., Iskanderani F. I. & Zared A. H. (1991). Hydrogen effects in a dual-phase microalloy steel, *Journal of Materials Science, Volume 26*, 5644-5654p.
- [96] Park J. S., Lee J. W., Hwang J. K. & Kim S. J. (2020). Effects of alloying elements (C, Mo) on Hydrogen Assisted Cracking Behaviors of A516-65 Steels in Sour Environment, *Materials (Basel)*, 13(18): 4188, doi: 10.3390/ma13184188
- [97] Caskey Jr. G. R. (1983). Hydrogen compatibility handbook for stainless steels, Technical report: *Du Pont de Nemours (E.I.) and Co., Aiken, SC (United States). Savannah River Lab.*
- [98] Depover T., Laureys A., Escobar D. P., Van den Eeckhout E., Wallaert E. & Verbeken K. (2018). Understanding the interaction between a steel Microstructure and Hydrogen, *Materials (Basel)*, 11(5): 698, doi: 10.3390/ma11050698
- [99] Nanninga N. E. (2005). Effects of microstructure and alloying elements on the resistance of fastener grade steels to hydrogen assisted cracking, *Dissertation, Master's Theses and Master's Reports, Michigan Technological University*, <https://doi.org/10.37099/mtu.dc.ets/24>
- [100] Martin M. L., Connolly M. J., DelRio F. W. & Slifka A. J. (2020). Hydrogen embrittlement in ferritic steels. *National Institute of Standards and Technology, US Department of Commerce, PMC, Appl Phys Rev*; 7(4): doi: 10.1063/5.0012851
- [101] Pu S. D., Turk A., Lenka S. & Ooi S.W. (2019). Study of hydrogen release resulting from the transformation of austenite into martensite, *Materials Science and Engineering: A, Volume 754*, 628-635p.

- [102] Chang C. (2010). Correlation between the microstructure of Dual Phase Steel and Industrial Tube Bending Performance, *Electronic Theses and Dissertation*. 178. <https://scholar.uwindsor.ca/etd/178>.
- [103] Tasan C.C., Diehl M., Yan D. Bechtold M., Roters F., Schemmann L., Zheng C., Peranio N., Ponge D., Koyama M., Tsuzaki K. & Raabe D. (2015), An Overview of Dual-Phase Steels: Advances in Microstructure-Oriented Processing and Micromechanically Guided Design, *Annual Review of Materials Research*, Volume 45:391-431p, <https://doi.org/10.1146/annurev-matsci-070214-021103>.
- [104] Xu Y., Dan W., Ren C., Huang T. & Zhang W. (2018). Study of the Mechanical Behavior of Dual-Phase Steel Based on Crystal Plasticity Modeling Considerin Strain Partitioning, *Metals* 2018, 8(10), 782; <https://doi.org/10.3390/met8100782>
- [105] Allam T., Guo X., Lipińska-Chwałek M., Hamada A., Ahmed E. & Bleck W. (2020). Impact of precipitates on the hydrogen embrittlement behavior of a V – alloyed medium-manganese austenitic stainless steel, *Journal of Materials Research and Technology*, Volume 9, Issue 6, 13524-13538p, ISSN 2238-7854, <https://doi.org/10.1016/j.jmrt.2020.09.085>.
- [106] Brahim S.V., Yue S. & Sriraman K. R. (2017). Alloy and composition dependence of hydrogen embrittlement susceptibility in high-strength steel fasteners, *The Royal Society Publishing*, <https://doi.org/10.1098/rsta.2016.0407>
- [107] Van der Eijk C., Haakonsen F., Klevan O. S. & Grong Ø. (2011). Development of grain refiner alloys for steels, *AISTech-Iron and Steel Technology Conference Proceedings*, 559-566, <https://researchgate.net/publication/287869703>.
- [108] Claeys L., De Graeve I., Depover T. & Verbeken K. (2020). Hydrogen-assisted cracking in 2005 duplex stainless steel: Initiation, propagation and interaction with deformation-induced martensite, *Materials Science and Engineering: A*, Volume 797, 140079p, ISSN 0921-5093, <https://doi.org/10.1016/j.msea.2020.140079>.
- [109] Koyama M., Akiyama E., Lee Y. K., Raabe D. & Tsuzaki K. (2017). Overview of Hydrogen Embrittlement in High-Mn Steels, *International Journal of Hydrogen Energy*, <https://www.sciencedirect.com/science/article/pii/S0360319917308418>
- [110] Hatlevik Ø., Gade S. K., Keeling M.K., Thoen P. M., Davidson A. P. & Way D. (2010). Palladium and palladium alloy membrane for hydrogen separation and production: History, fabrication strategies,

and current performance, *Separation and Purification Technology*, Volume 73, Issue 1, 59-64p, ISSN 1383-5866, <https://doi.org/10.1016/j.seppur.2009.10.020>.

[111] Andreas D., Besim H., Zahra S., Klemensa M., Christof S. & Josef D. (2022). The role of hydrogen diffusion, trapping and desorption in dual phase steels, *Journal of Materials Science*, 4789-4805p, Volume 57, Issue 7. <https://doi.org/10.1007/s10853-021-06830-0>.

[113] Koyama M., Hirata K., Abe Y., Mitsuda A., Likubo S. & Tsuzaki K. (2018). An unconventional hydrogen effect that suppresses thermal formation of the hcp phase in fcc steels. *Scientific Reports:naturesearch*; 8: 16136. doi: 10.1038/s41598-018-34542-0

[114] Depover T., Hertelé S. & Verbeken K. (2019). The effect of hydrostatic stress on the hydrogen induced mechanical degradation of dual phase steel: A combined experimental and numerical approach, *Engineering Fracture Mechanics*, Volume 221, 106704p, ISSN 0013-7944, <https://doi.org/10.1016/j.engfracmech.2019.106704>.

Hydrogen evolution during directional solidification and its effect on porosity formation in aluminum alloys - Scientific Figure on ResearchGate. Available from: https://www.researchgate.net/figure/The-aluminum-hydrogen-phase-diagram-11_fig2_227259863 [accessed 7 Sep, 2023]

[115] Vucko F., Ootsuka S., Rioual S., Diler E., Nazarov A. & Thierry D. (2022). Hydrogen detection in high strength dual phase steel using scanning Kelvin probe technique and XPS analyses, *Corrosion Science*, Volume 197, 110072p, ISSN 0010-938X, <https://doi.org/10.1016/j.corsci.2021.110072>.

[116] Flanagan T. B. & Oates W. A. (2019). Para-equilibrium Phase Diagrams, μ_H-X_M for Pd Alloy – H systems, *Phase Equilibrium Diffusion*. 40:285-290p, <https://doi.org/10.1007/s11669-019-00724-0>.

[117] Wipf H. (). Solubility and diffusion of hydrogen in pure metals and alloys. *IOP Publishing ltd, Physica Scripta*, Volume 2001, Number T94, doi 10.1238/Physica.Topical.094a00043.

[118] Wille G. W. & Davis J. W. (1981). Hydrogen in titanium alloys. United States: N. p., 1981. Web. doi:10.2172/6420120.

[119] Xi X., Wu T., Tian Y., Hu J., Huang S., Xie T., Wang J. & Chen L. (2023). The role of reverted transformation in hydrogen embrittlement of a Cu-containing low carbon high strength steel., *Journal of Materials Research and Technology*, Volume 25, 5990-5999p, ISSN 2238-7854, <https://doi.org/10.1016/j.jmrt.2023.07.071>.

- [120] Wang Z., Lui J., Huang F., Bi Y. & Zhang S. (2020). Hydrogen Diffusion and its Effect on Hydrogen Embrittlement in DP Steels With Different Martensite Content, *Front. Material: Sec. Structural Materials*, Volume 7 <https://doi.org/10.3389/fmats.2020.620000>
- [121] Pietrzyk M. and Kuziak R. (2012) “6 - Modelling phase transformations in steel,” in Woodhead Publishing Series in Metals and Surface Engineering, J. Lin, D. Balint, and M. B. T.-M. E. in M. F. P. Pietrzyk, Eds. Woodhead Publishing, 2012, pp. 145–179
- [122] Zhao J. and Jiang Z. (2018), “Thermomechanical processing of advanced high strength steels,” *Prog. Mater. Sci.*, vol. 94, pp. 174–242, 2018, doi: <https://doi.org/10.1016/j.pmatsci.2018.01.006>.
- [123] Loidl M. (2014) , Entwicklung einer Prüfmethode zur Charakterisierung höchstfester Karosseriestähle hinsichtlich des Risikos zur Wasserstoff induzierten Rissbildung. PhD thesis, Universität Stuttgart, 2014.
- [124] Drexler A., Helic B., Silvayeh Z., Mraczek K., Sommitsch C. & Domitner J. (2022). The role of hydrogen diffusion, trapping and desorption in dual phase steels. *Journal of Materials Science: 4789-4805pp*, Volume (57), Issue 7.